



Development of a data-driven semi-distributed hydrological model for regional scale catchments prone to Mediterranean flash floods

M. Adamovic, F. Branger, Isabelle Braud, S. Kralisch

► To cite this version:

M. Adamovic, F. Branger, Isabelle Braud, S. Kralisch. Development of a data-driven semi-distributed hydrological model for regional scale catchments prone to Mediterranean flash floods. *Journal of Hydrology*, 2016, Flash floods, hydro-geomorphic response and risk management, 541 (Part A), pp.173–189. 10.1016/j.jhydrol.2016.03.032 . hal-02084519

HAL Id: hal-02084519

<https://hal.science/hal-02084519>

Submitted on 16 May 2020

HAL is a multi-disciplinary open access archive for the deposit and dissemination of scientific research documents, whether they are published or not. The documents may come from teaching and research institutions in France or abroad, or from public or private research centers.

L'archive ouverte pluridisciplinaire **HAL**, est destinée au dépôt et à la diffusion de documents scientifiques de niveau recherche, publiés ou non, émanant des établissements d'enseignement et de recherche français ou étrangers, des laboratoires publics ou privés.

Development of a data-driven semi-distributed hydrological model for regional scale catchments prone to Mediterranean flash floods

M. Adamovic^{1,2}, F. Branger¹, I. Braud¹, S. Kralisch³

[1] Irstea, UR HHLY, Hydrology-Hydraulics Research Unit, Lyon-Villeurbanne, France

[2] CNRS-IRD, HydroSciences Laboratory, Place Eugene Bataillon, 34095 Montpellier, France

[3] Department of Geoinformatics, Hydrology and Modeling, School of Chemical and Earth Sciences, Friedrich-Schiller-University, Jena, Germany

Correspondence to: M. Adamovic (marko.adamovic@hotmail.com)

Abstract

Flash floods represent one of the most destructive natural hazards in the Mediterranean region. These floods result from very intense and spatially heterogeneous rainfall events. Distributed hydrological models are valuable tools to study these phenomena and increase our knowledge on the main processes governing the generation and propagation of floods over large spatial scales. They are generally built using a bottom-up approach that generalizes small-physics representations of processes. However, top-down or data-driven approach is increasingly shown to provide also valuable knowledge. A simplified semi-distributed continuous hydrological model, named SIMPLEFLOOD, was developed, based on the simple dynamical system approach (SDSA) proposed by Kirchner (WRR, 2009, 45, W02429), and applied to the Ardèche catchment in France (2388 km²). This data-driven method assumes that discharge at the outlet of a given catchment can be expressed as a function only of catchment storage. It leads to a 3-parameter nonlinear model according to rainfall and runoff observations. This model was distributed over sub-catchments and coupled with a kinematic wave based flow propagation module. The parameters were estimated by discharge

1 recession analyses at several gauged stations. Parameter regionalization was conducted using a
2 Factorial Analysis of Mixed Data (FAMD) and Hierarchical Classification on Principal Component
3 (HCPC) in order to find relationships between the SDSA approach and catchments characteristics.
4 Geology was found to be the main predictor of hydrological response variability and model
5 parameters were regionalized according to the dominant geology. The SIMPLEFLOOD model was
6 applied for a 12-year continuous simulation over the Ardèche catchment. Four flash flood events
7 were also selected for further analysis. The simulated hydrographs were compared with the
8 observations at 11 gauging stations with catchment size ranging from 17 to 2300 km². The results
9 show a good performance of the model for the continuous and flash flood events occurring under wet
10 conditions, whereas the model underestimates discharge for events occurring after a long dry period.
11 The simple modelling approach provided interesting insight into the Ardèche catchment functioning
12 and offers perspective for a better simulation of flash floods, mainly under wet conditions.

1. Introduction

Catchments in the Mediterranean basin are prone to a large number of devastating events sometimes followed with loss of life and high economic and social impact (Gaume et al., 2009). Due to its geographic position with many surrounding mountains, the Mediterranean basin is usually exposed to typical convective mesoscale systems leading to heavy precipitation and thus to flash floods. These events occur especially during fall and winter periods as remarked by Borga and Morin (2014). In addition to its specific position, the Mediterranean basin is also pointed out as one of the “hot-spots” in future climate change predictions (Giorgi, 2006). This could lead eventually to more frequent and more intense extreme events. The study of the water cycle in such Mediterranean conditions, as well as a better understanding and modelling of processes triggering flash floods, are central research topics for instance addressed in the HyMeX¹ (Hydrological Cycle in the Mediterranean Experiment, Drobinski et al. (2013)) program and in the FloodScale² project (Braud et al., 2014), to which this study contributes.

There are lots of operational models developed in order to deal with flash floods on the catchment scale (up to hundreds of square kilometers). In Mediterranean context, many models such as TOPMODEL (Beven, 2012) and its versions (Saulnier and Le Lay, 2009; Vincendon et al., 2010), SCS based models (e.g. (Gaume et al., 2004; Sangati and Borga, 2009; Rozalis et al., 2010), modeling approaches including infiltration excess and sub-surface flow such as the MARINE model (Roux et al., 2011; Garambois et al., 2013), rainfall-runoff flash flood models based on Green-Ampt infiltration method (Zanon et al., 2010), geomorphological approaches (*Continuum* model, Silvestro et al., 2011; 2013), and runoff threshold methods (e.g. Gourley et al., 2014) have been used for flood prediction of small to medium size basins.

¹ www.hymex.org

² <http://floodscale.irstea.fr/>

As noted by Hapuarachchi et al. (2011) in their review of flash flood forecasting, even though there are many existing models working on these scales, there is still no clear consensus which model is preferable and which is not. In the regional scale catchments (some 1000 km²), models able to simulate flash floods are poorly described or do not exist in the literature.

The approach developed in this study aims at providing increased knowledge of dominant hydrological processes during flash floods in the Mediterranean context by combining data analysis and distributed hydrological modeling. By better understanding dominant hydrological processes and their drivers, this work could improve the models used operationally for flash flood forecasting and warning, in particular in ungauged catchments, through a better integration of process knowledge in model structure or parameters specification. In the context of Mediterranean flash floods caused by intense and localized rainfall events, it is particularly important to take into account spatially distributed rainfall (Sangati and Borga 2009; Anquetin et al., 2010; Trambly et al. 2010; Zocatelli et al., 2010). Therefore, distributed modeling approaches can be suited to flash flood simulations on regional scale catchments.

Distributed hydrological models are generally built using a bottom-up approach (Sivapalan, 2003b; Zehe et al., 2006), following the blueprint proposed by Freeze and Harlan (1969). These types of models generalize small-physics representations of processes by using for example Darcy or Richards' equations (Bloschl and Sivapalan, 1995; Kirchner, 2006). Their use to describe processes at larger scales leads to the calibration of “effective parameters” which are sometimes difficult to link with measurable quantities (Sivapalan, 2003b). Recent methods showed that combining the use of small-scale variability and regionalization techniques can be still efficient in preserving spatial patterns of variability (Samaniego et al., 2010). Use of distributed hydrological models for process understanding during flash floods in the Mediterranean region is more recent. Examples of such studies are those of Bonnifait et al. (2009), Manus et al. (2009), Braud et al. (2010) and Vannier (2013) which are based on a reductionist approach to gain insight into active hydrological processes

during floods and highlight a lack of data or parameter information. Other examples are also models used to simulate landslides triggered by flash floods in the Mediterranean region (Bathurst et al. 2006; Frattini et al., 2009).

However, top-down or data-driven approach is increasingly shown to provide also valuable knowledge. Klemeš (1983) was one of the first hydrologists proposing the use of this method. Top-down approach promotes a combination of data analysis and process conceptualization (Kirchner, 2009; Sivapalan, 2003b). The obtained models are simple and with a limited number of parameters that can be estimated from the available data. The data-based approach proposed by Kirchner (2009) is adopted in this study. It was successfully applied at several gauged stations during low vegetation periods (November-March; Adamovic et al., 2015) in the Ardèche catchment, France. This data-driven method assumes that discharge at the outlet of a given catchment can be expressed as a function of catchment storage only and determines a 3-parameter nonlinear model according to rainfall and runoff and recordings. For developing distributed hydrological models, it will be essential to identify links between the parameters and catchment characteristics, including physiographic and hydro-climatic factors in order to regionalize the parameters since the Mediterranean catchments are characterized by heterogeneous topography, vegetation and geology.

Catchment classification has been put forward as a useful tool to deal with high spatial, temporal and process variability (McDonnell and Woods, 2004) and bring some harmony to the cacophony presented in hydrology (Sivapalan, 2003a). Wagener et al. (2007) in their review of classification techniques highlight how such a classification framework would contribute to understanding of how catchment structure and climate region define catchment function pattern. The ultimate goal of classification is to relate catchment structures to hydrologic response characteristics (Wagener et al., 2007) by combining catchment “form” (e.g. geologic characteristics) and climate forcing (Winter, 2001) and thus signatures of runoff response. Winter suggested that catchments with similar geology, topography (slope) and climate regime would have similar flow paths regardless of the catchment

distance. In their review, Wagener et al. (2007) distinguished classification based on catchment structure, classification based on hydro-climatic region and classification based on functional response. In the last years in order to classify catchments, a significant contribution to this domain has been made by using self-organizing maps (Herbst et al., 2008; Ley et al., 2011; Toth, 2013), Bayesian clustering (Sawicz et al., 2011), local variance reduction method (He et al., 2011), Principal Component (PCA) and Canonical Correlation Analysis (CCA) (Di Prinzio et al., 2011) and many others. For instance Sawicz et al. (2011) used cluster analysis of runoff coefficients and slope of flow duration curve to classify 300 catchments into 9 groups. Similarly, using four signatures (the aridity index, the seasonality index, day of peak precipitation and day of peak runoff) Coopersmith et al. (2012) showed that 300 catchments can be grouped into 6 classes. These works provided a glimpse of the first order differences between catchments. Furthermore, Yaeger et al. (2012) in their work pointed out that climate seasonality and aridity are the main controls of flow regime in the central part of the flow duration curve. They argued that catchment characteristics such as soil represent dominant control in the low-flow tail of the regime curve. All these works made a huge step forward in distinguishing catchment characteristics as the drivers of simple hydrological process descriptions at the catchment scale and will be further used in this study.

In this study, the SIMPLEFLOOD hydrological model is designed that provides a distributed and data-driven modeling of regional scale catchments. The model is based on the simple dynamical systems approach. It simulates and predicts hydrological behavior throughout the year, especially during flash floods. Due to its simplicity the model is named SIMPLEFLOOD.

The study area is the Ardèche catchment (2388 km²), which is typical of Mediterranean catchments with highly variable rainfall, steep slopes, and heterogeneous geology and pedology. It is one of the studied catchments of the Cévennes-Vivarais Hydro-Meteorological Observatory (OHM-CV, Boudevillain et al. (2011)).

In the present paper, focus is given on the following questions: 1/ how can the simple dynamical system approach (SDSA) be translated into a distributed hydrological model concept in a Mediterranean type catchment like the Ardèche with its particular conditions (size, climate, geological and pedological heterogeneity)? 2/ what are the dominant predictors of hydrological variability that can serve as a basis for parameter regionalization? 3/ what is the performance of such a model, run without specific calibration, in reproducing observed discharge dynamics?

In Section 2, the model concepts and implementation is presented. The case study of the Ardèche catchment and the available data are presented in Section 3. Section 4 deals with the model setup and presents the methodology that is used to regionalize the parameters of the SDSA approach on ungauged catchments. Finally, the simulation results for continuous simulations and selected major flood events are presented in Section 5 and discussed in Section 6.

2. Model description

2.1 Simple dynamical systems approach-SDSA

Kirchner (2009) proposed a method for determining non-linear reservoir parameters for a simple bucket model with the assumption that discharge Q can be expressed uniquely as a function of total water storage S in the catchment. Many studies have been successfully conducted using this approach (Teuling et al, 2010; Brauer et al., 2013, Melsen et al., 2014, Adamovic et al., 2015). They all had good results in low-vegetation (i.e. when deciduous trees have lost their leaves) and wet periods.

The most important feature of the SDSA approach is the so called discharge sensitivity function $g(Q)$. It describes the sensitivity of discharge to changes in storage, as a function of discharge itself. This is useful because discharge is directly measurable whereas whole-catchment storage is generally not, as integrated approaches such as the use of gravity measurements, for instance using the GRACE

(Gravity Recovery And Climate Experiment) satellite data only provide estimates for large scale catchments (Reager et al., 2009).

The $g(Q)$ function is estimated during the periods when precipitation and actual evapotranspiration are relatively small compared with discharge (Kirchner, 2009), obtaining the following equation, which shows that under these conditions the discharge sensitivity function can be estimated from discharge data alone:

$$g(Q) = \frac{dQ}{dS} \approx -\frac{dQ/dt}{Q} \Big|_{P \ll Q, AET \ll Q} \quad (1)$$

where $g(Q)$ is the sensitivity function, P is precipitation, AET is actual evapotranspiration, Q is discharge, S is catchment water storage and dQ/dt is a rate of change of discharge over time (t).

More precisely, the sensitivity function $g(Q)$ is estimated using discharge records from low-vegetation periods when vegetation and ET_0 could be considered to have a smaller impact on stream discharge (Adamovic et al., 2015). This is essential in order to have a robust $g(Q)$ function where the mass balance of the catchment is dominated by discharge and where the relationship is not distorted by evapotranspiration.

This leads to the following expression in log space where an approximation using a quadratic function is proposed:

$$\ln(g(Q)) = \ln\left(-\frac{dQ/dt}{Q} \Big|_{P \ll Q, AET \ll Q}\right) \approx C_1 + C_2 \ln(Q) + C_3 (\ln(Q))^2 \quad (2)$$

where C_1 , C_2 and C_3 are parameters of a quadratic function on $\ln(-dQ/dt)$ versus $\ln(Q)$ plot (Kirchner, 2009). In the remaining of the paper, we will refer to those parameters as “recession parameters”, although they are not estimated using all the recessions data, but only the values where P and AET can be considered as negligible.

This method is simple enough so that it enables the derivation of a continuous rainfall-runoff modelling approach, that can be applied for the whole time period and not only for the periods where

the $g(Q)$ function has been estimated. This model is given by the following equation (Kirchner, 2009):

$$\frac{d(\ln(Q))}{dt} = \frac{1}{Q} \frac{dQ}{dt} = \frac{g(Q)}{Q} (P - AET - Q) = g(Q) \left(\frac{P - AET}{Q} - 1 \right) \quad (3)$$

This equation is a first-order nonlinear differential equation used for discharge simulation directly from P and AET time series. Discharge is computed using fourth-order Runge-Kutta integration, iterating on an hourly time-step where a single value of measured discharge is used to initialize the simulation.

To estimate the AET term in Eq. (3), it is assumed, in the present study, that actual evapotranspiration is equal to potential evapotranspiration (PET) throughout the year, being defined as reference evapotranspiration ET_0 modulated by a monthly crop coefficient depending on the nature of vegetation for each catchment. The strong hypothesis that $AET = PET$ is likely to be more relevant in winter, when there is sufficient water content in the air and soils, than in summer. Nonetheless this assumption is used, even in summer, as a first rough approximation in order to assess the feasibility of such a simple modeling concept.

2.2 Design and implementation of SIMPLEFLOOD

In order to combine the distributed modeling approach with the SDSA approach which is defined at the catchment scale, the spatial modeling units chosen for SIMPLEFLOOD consist of sub-catchments. Climate forcing (precipitation and reference evapotranspiration) should be allocated to each sub-catchment. Each sub-catchment must be homogeneous enough, consistently with the Hydrological Response Unit (HRU) concept (Flügel, 1995), so that clear descriptors can be identified. The size of the modeling units will be therefore constrained by the local climate conditions, such as the typical spatial structure of storm events, and by the heterogeneity of the geographic descriptors of the catchment, such as land use or geology. Runoff is generated on each

modeling unit according to the SDSA approach. In order to transfer the flow to the catchment outlet, SIMPLEFLOOD also incorporates a routing algorithm in the river network. As not all the modeling units are gauged, parameter regionalization will be necessary to distribute the parameter sets of the $g(Q)$ function derived on gauged sub-catchments when P and AET can be considered as negligible.

SIMPLEFLOOD was implemented in the JAMS modeling framework (Kralisch and Krause, 2006), which is developed at the Department for Geoinformatics, Hydrology and Modeling of the Friedrich-Schiller-University Jena, in Germany. Like other modeling platforms, JAMS is able to integrate numerous process components (modules) of the user's choice, while providing support for non-hydrology-specific tasks such as data input/output management and runtime management.

The JAMS modeling framework contains already many implemented models such as the process-oriented model J2000 (Krause et al., 2006), water balance model J2000g (Krause and Hanisch, 2009), process oriented nutrient transport model J2000s (Fink et al., 2007) and many components aimed at land use management assessment. SIMPLEFLOOD reuses components from the J2000 model, while incorporating a new component that implements the SDSA approach (see Figure 1). Thus SIMPLEFLOOD consists of:

1. Parameter input and initialization
2. Climate forcing reading (ET_0 and P)
3. Regionalization of climate data
4. Potential evapotranspiration (PET) calculation
5. Runoff production
6. Flow routing

Regionalization in Step 3 is based on the Inverse Distance Weightings (IDW) method like in the J2000 model. The detail description of how this component works can be found in the JAMS wiki³.

³ http://jams.uni-jena.de/ilmswiki/index.php/Hydrological_Model_J2000

The definition of the number of stations that are nearest to the particular sub-catchment and the weightings of those n stations calculated via IDW dependently on their distances for each sub-catchment are taken into account. Regionalization is used for ET_0 as shown in Table 1. For rainfall, average rainfall at the scale of the sub-catchment was used as direct input of the model.

In step 4, it is assumed that $PET = ET_0 \times Kc$. In order to calculate potential evapotranspiration in SIMPLEFLOOD model, values of reference evapotranspiration and crop coefficients are needed. This is achieved by the redistribution of crop coefficient to each sub-catchment, according to landuse. Then, a potential evapotranspiration is calculated at each time step and for each sub-catchment by multiplying reference ET_0 and the crop coefficient of the current month.

	Model component	Component description	Input data and/or parameters
Parameter input	EntityReader	Reads sub-catchments and reaches	Reach and sub-catchment files Obtained by GIS pre-processing
	LUReader	Reads monthly crop coefficient (Cr) according to the dominant land-use	$Kc_1, Kc_2, \dots Kc_12$ in file
	GReader	Reads “recession parameters”	C_1, C_2 and C_3 in file (obtained from $g(Q)$ estimation and regionalization)
Input	Model initialization	Reads the initial value of discharge	Q_{init} (obtained as a specific discharge at the catchment outlet)
Input	TS input	Reads time-series data	P, ET_0
	ET_0 regionalization	Regionalize ET_0 for each sub-catchment	n (number of stations), W (weightings)
	PET calculation	Calculates PET for each sub-catchment	$AET = PET = ET_0 \times Kc$
	Runoff production	Calculates discharge for each sub-catchment	$Q_{init}, C_1, C_2, C_3, AET, P$
	Flow routing	Transfer the water from one reach to the next one	Reach length (l), slope (α), width (b) and roughness (μ)

Table 1. Input data and parameters for SIMPLEFLOOD

In step 5, the model outputs are the discharge time series at the outlet of each modeling unit (sub-catchment). These discharges are routed as inflow in each river reach in step 6. The Reach routing component takes care of flow routing in the reach network using a variant of kinematic wave approach and assuming rectangular channel geometry. In each reach, water velocity is computed according to Strickler coefficient and then the water is passed to the next downstream reach based on the velocity and length of the reach. The corresponding parameters are reach length, slope, width and roughness. SIMPLEFLOOD runs at the hourly time step.

3. Case study

3.1 The Ardèche catchment

The Ardèche catchment is located in southern France. The catchment has an area of 2388 km², and the Ardèche river itself has a length of 125 km. Elevation ranges from the mountains of the Massif Central (highest point: 1681 m) in the northwest, to the confluence with the Rhone River (lowest point: 42 m) in the southeast (Figure 2).

The main lithologies found in the Ardèche are schist, granite, and limestone. For a more detailed geological description see Adamovic et al. (2015) and Naulet et al. (2005). Figure 3 shows the geology of the Ardecche and surrounding area.

Among the land use types found in the Ardèche, forest dominates throughout the basin according to the land use map derived by J. Andrieu (Univ. Nice) from Landsat 30m satellite images⁴. Forest is represented by a mix of coniferous (27%), broadleaf (13%) and Mediterranean trees (17%). Shrubs and bushes are also well represented in the catchment, occupying a significant portion of the area (17%). Also significant areas of bare soil are distinguished in the central and southern part of the

⁴ http://mistrals.sedoo.fr/?editDatsId=1377&datsId=1377&project_name=HyMeX&q=land+use

Ardèche, as well as a few small urban areas and areas of early (e.g. carrots, celery, lettuce, radish, peas) and late crops (e.g. spinach, eggplant, sugar beet).

There is a strong influence of the Mediterranean climate with seasonally heavy rainfall events during autumn. Historical data show that these events usually lead to flash floods (Lang et al., 2002). Lang et al. also comment on the relatively quick flow response (a couple of hours) to precipitation due to the steepness of the upstream part of the catchment and presence of granitic and basaltic rocks.

The hydrological year consists mainly of two periods. There is a rainy season (September-February) with maximum precipitation intensity in autumn, characterized by rainfall amounts greatly exceeding reference evapotranspiration ET_0 (calculated based on the SAFRAN reanalysis of Quintana-Seguí et al. (2008)), and by high discharge. On the other hand, during the dry season (March-August), on average ET_0 is much larger than precipitation and runoff is low.

In the Ardèche basin there are numerous dams (Figure 2) built along the upstream Chassezac river, and additional water input in the upstream Ardèche coming from the neighbourhood Loire catchment (Montpezat hydropower plant). There are also numerous summer agricultural uptakes along the Baume River. All this influences strongly the natural streamflow downstream. On Figure 2, thus influenced and non-influenced gauging stations are distinguished.

3.2 Available data

In the Ardèche catchment, measurements of the hydrological state variables have mainly been started in the 1960s for the purpose of flood forecasting. In this study, hourly data of precipitation (P), reference evapotranspiration (ET_0) and discharge (Q) from the period 1 Jan 2000 until 31 Dec 2012 are used.

Discharge data come from operational networks, and not from research catchments as in previous applications of the SDSA as already discussed in Adamovic et al. (2015). They are obtained from the national Banque Hydro website (www.hydro.eaufrance.fr) and Electricité de France

(www.france.edf.com/). Figure 2 and Table 2 present the data that were used in this study. Criteria for the selection of stations were the availability of data for the above mentioned time frame, and sufficient quality of stations and rating curves, as indicated by data managers. In particular, stations that presented bad low flow quality are discarded (due either to undocumented agricultural uptakes or very uncertain low flow rating curves) in order to compare the model output with more reliable water balance estimates. For dam-influenced downstream gauging stations of the Ardèche River, "natural" or partially dis-influenced time series could be reconstructed at the daily time step in the framework of the Floodscale project (Noël, 2014). At the hourly time step, it is considered that the influence of dams is negligible during flood events when it is overflowing and releasing the water. On another side, the daily turbine flows of the Chassezac dams were not available, making the dis-influence calculations downstream of Chassezac river only partial (see Table 2). When these data are available, a much more precise and general picture about water balance in the Ardèche can be assessed.

N°	Station name	Catchment area (km ²)	Station alt. (m)	Influenced by dam operations
1	<i>Ardèche at Meyras</i>	98	318	No
2	<i>Borne at Nicoulaud</i>	62.7	617	No
3	<i>Thines at Gournier</i>	16.7	415	No
4	<i>Altier at Goulette</i>	103	628	No
5	<i>Ardèche at Pont-de-Labeaume</i>	292	295	Yes
6	<i>Ardèche at Ucel</i>	477	203	Yes
7	<i>Ardèche at Vogue</i>	623	143	Yes
8	<i>Baume at Rosieres</i>	210	148	partial
9	<i>Chassezac at Gravieres</i>	557	165	Yes
10	<i>Ardèche at Vallon-Pont-d'Arc</i>	2023	77	partial
11	<i>Ardèche at Sauze-Saint-Martin</i>	2257	46	partial
12	<i>Auzonnet at Mages</i>	49	355	No

Table 2- Presentation of the considered discharge gauging stations; stations used for parameter regionalization are highlighted in bold

SAFRAN precipitation reanalysis of Météo-France, based on 8 by 8 km² grids (Quintana-Seguí et al., 2008; Vidal et al., 2010) were used in this study. Data are derived using the results of a meteorological model that are constrained using existing Météo-France rain gauges. To compute the reference evapotranspiration ET_0 , the climate variables of the SAFRAN reanalysis of Météo-France at

an hourly time step were also used. ET_0 is calculated using the Penman-Monteith formula according to FAO recommendations (Allen et al., 1998). Four major rainfall events were selected and looked at in more detail as presented in Section 3.3.

In the study, the BD CARTHAGE® database of drainage network (Figure 2) is used. Table 2 presents the 11 sub-catchments in the Ardèche that are included in this study plus additional non-disturbed catchment (#12) located in a limestone area. For non-influenced stations (in bold in Table 2) topographic variables using a 25-m resolution DEM and TAUDDEM tool 5.2 (Tarboton, 1997) were computed in ARCGIS 10.2 software. Five variables such are: (i) *drainage area*; (ii) *average altitude*; (iii) *average slope*; (iv) *channel length*; and (v) *drainage density* were calculated. These variables are used in regionalization analysis and are presented in Section 4.

3.3 Selected flash flood events

Four major events occurring during the 2000-2012 period were selected in this study. Figure 4 presents the events cumulated rainfall, averaged over the SIMPLEFLOOD model mesh (see section 4.2 for the model set up).

The December 2003 flood event produced the maximum peak flow of the examined period (2000-2012) of 2960 m³/s at the Sauze-Saint-Martin station (#9). The event lasted a couple of days (from 30/11 until 04/12) with maximum intensities reached on second and third December 2003. The event produced high flows at Ardèche at Vogue (#7) with maximum observed discharge of 1120 m³/s. During this event it rained over the whole Ardèche (average accumulation of 285 mm).

Two important successive precipitation extreme events occurred in the Ardèche catchment at the end of October (average catchment accumulation of 165 mm) and beginning of November 2008 (rainfall accumulation of 260 mm). The first event occurred between the 19th and 23rd of October reaching its maximum intensities on October 21st and 22nd. The cumulative precipitation of this five days event is spatially variable across the Ardèche catchment with maximum precipitation in the central part of the

catchment. The second event occurred some days after, more precisely between 31/10/2008 and 06/11/2008 with maximum intensities on November 1st and 2nd. It generated large precipitation accumulations over localized areas in the north-west and south-west of the Ardèche mountain ridges. This seven day event lasted longer than the previous one with maximum precipitation amount of 600 mm, recorded in the local station Altier. A maximum discharge of $2450 \text{ m}^3 \text{ s}^{-1}$ on November 2nd was recorded at the Sauze-Saint-Martin station (#12).

In November 2011, a significant precipitation accumulation occurred in the Ardèche catchment over the mountainous areas in the western part of the catchment (average accumulation of 375 mm). This event occurred between 1st and 6th of November 2011 with maximum precipitation recorded on November 3rd and 4th in the upstream catchments. The event produced high flows along the Ardèche and Chassezac rivers with flow of $1860 \text{ m}^3/\text{s}$ at the catchment outlet.

Figure 5 shows the measured instantaneous specific peak discharge as function of catchment area for the four selected events. The figure shows that the hydrological response was quite similar at all scales for the December 2003 event with specific peak discharge of about $2 \text{ m}^3 \text{ s}^{-1} \text{ km}^{-2}$ for catchments size ranging from about 20 to 2000 km^2 . The October 2008 event is less intense at small scales, due to rainfall heterogeneity, but maximum specific peak discharge is larger than $1 \text{ m}^3 \text{ s}^{-1} \text{ km}^{-2}$ at the outlet and in medium sized catchments. Finally the November 2008 and 2011 events follow more classical patterns with higher values of specific peak discharge for smaller catchments and a general decrease when catchment size increases. In all cases, the increase of discharge at the outlet occurring in less than 24 hours and the range of specific discharge clearly show that these events are flash floods as defined by Gaume et al. (2009) or Braud et al. (2014).

4. Parameter regionalization, model set up and evaluation

4.1 Parameter regionalization using the FAMD and HCPC classification

The parameters for which a regionalization method was applied are the three “recession parameters” C_1 , C_2 and C_3 for which estimations are available at the gauged catchments and for which a value is required for each modelling units. Several explanatory factors, detailed in section 4.1.3 were used to achieve this regionalization.

4.1.1 Selection of the regionalization method

Classification techniques were shown to be efficient in providing information about catchment functioning. In this analysis the different types of variables related to catchment structure, to catchment hydro-climatic conditions and to catchment functioning are retained in order to find relationships between those variables and recession parameters.

As will be shown more in details later, this led to define both quantitative variables (such as catchment area, slope or altitude) and qualitative variables (geology, landuse). Quantitative variables are generally dealt with using Principal Component Analysis (PCA), whereas categorical variables are handled using Multiple Correspondence Analysis (MCA). For mixed data, and in order to use as much as possible all the available information Factor Analysis of Mixed Data (FAMD) was introduced (e.g. Pagès (2004)). FAMD analyses are preferable and appropriate in two cases as Pagès (2004) suggested:

- *Case study when there are a few qualitative variables compared with quantitative ones*
- *Case study when the number of individuals is low (less than 100).*

As those two conditions are fulfilled in this case study, FAMD is retained as an appropriate method in the analysis. To enhance FAMD results, a Hierarchical Clustering of Principal Components was further applied.

4.1.2 Principles of the FAMD

Principles of Factor Analysis of Mixed Variables are described in Pagès (2004). A simplified description can be found in Wikipedia⁵.

In the analysis, the representation of individuals is made directly from factors as a projection on the first two dimensions. The representation of quantitative variables is constructed as in PCA (correlation circle). The representation of the categories of qualitative variables is as in MCA: a category is at the centroid of the individuals who possess it. One of the important indicators that gives the quality of representation of a variable (e.g. slope) is \cos^2 . It is measured by the squared cosines between the vector issued from the variable position and its projection on the axis (Le et al., 2008) where values close to 1 mean that the variable is well projected.

After the FAMD analysis is conducted, the classification of individuals is then established using a hierarchical classification on principal components (HCPC), i.e. using individual coordinates on principal components as a basis for classification. The HCPC method enables to classify the individuals into homogeneous groups (*Ward criteria*). Usually it is used as complement to factor analyses. The algorithm groups the closest individuals on the factorial map in pairs, then aggregates the closest groups in pairs until reaching the proposed level of clustering.

Eventually, having defined the groups of individuals, the next step in analysis is to test whether the individual varies according to each homogeneous area. This is achieved by analyzing the variance (one-way ANOVA) to test for significant differences in catchments between each determined group/cluster. All statistical analyses (FAMD, HCPC) were performed with R programming language using the FactoMineR package⁶.

⁵ https://en.wikipedia.org/wiki/Factor_analysis_of_mixed_data

⁶ <http://factominer.free.fr/index.html>

4.1.3 Application to our case study

The FAMD was applied to the four gauged sub-catchments in the Ardèche already studied in Adamovic et al. (2015) and the Auzonnet catchment located nearby (see Figure 3). This catchment was also sampled for the analysis since it is located on different geological conditions (limestones) and there is no dam that disturbs its water balance as in Ardèche. It drains an area of 49 km² and is predominantly characterized by different types of sedimentary rocks. Recession analyses were also successfully applied there (see Adamovic, 2014).

In order to increase the number of individuals, parameters estimated in different vegetation growth conditions were taken into account. These conditions include all year periods, low-vegetation and vegetation 2000-2008 periods. Vegetation periods include the periods between 1 of April and 30 of October of each year. Low-vegetation periods include the time frame between 1 of November and 31 of March.

Five groups of explanatory predictor variables were used: **topographic variables** ((i) *area*; (ii) *average altitude*; (iii) *Strahler number*; (iv) *average slope*; (v) *drainage density*; and (vi) *total channel length*), **land use, geology, meteorological variables** ((i) *runoff coefficient C*, (ii) *ratio of potential evapotranspiration ($KcET_0$) and precipitation PET/P* , and (iii) *mean annual precipitation P_{avg}* for all year, vegetation and low-vegetation period between 2000-2008), and **recession parameters** (C_1 , C_2 , C_3) as explained estimated variables. The factors used as explanatory variables act as a fingerprint of the catchment since they incorporate many aspects of runoff generation controls such as soils, geology, topography and land use, and hydro-climatic characteristics.

Three main land-use combination types were selected as predictor variables for FAMD analysis based on their predominance (dominance of first two land-use types):

1. **CM**- Coniferous-Mediterranean forest predominance
2. **CS**- Coniferous-Shrubs predominance

3. *CLC*- Coniferous-Late crops predominance

The dominant geologies were categorized as *granite*, *schists/basalts* and *limestone*. The final set of variables used in this study is presented in Table 3.

It can be noted that topographic variables along with geology and land use will not change among the data sets. In order to constrain the conflicts that might appear in the statistical analysis; these variables are kept as explanatory ones and other variables were kept as active.

Catchment names	Area	Altitude	Strahler	Slope	Dd	L	C_1	C_2	C_3	Geology	Land use	C	Pavg	PET/P
1. The Ardèche at Meyras	98.43	898	4	23.43	0.96	94.31	-3.82	0.98	0.12	granite	CM	0.65	1621	0.5
2. Borne at Nicolaud Bridge	62.6	1113	3	20.13	0.95	59.26	-4.31	0.59	0.09	Schists	CM	0.76	2084	0.38
3. Thines at Gournier Bridge	16.73	893	3	16.72	0.81	13.51	-3.87	0.77	0.1	Granite	CS	0.63	1541	0.56
4. Altier at Goulette	103.42	1149	5	17.13	0.94	97.38	-3.88	0.95	0.07	Schists	CLC	0.66	1407	0.55
5. Auzonnet at Mages	49	355	3	14.9	0.36	17.6	-3.23	1.27	-0.49	limestones	CM	0.57	1137	0.78
6. The Ardèche at Meyras VEG	98.43	898	4	23.43	0.96	94.31	-3.56	0.89	0.09	Granite	CM	0.41	1361	0.87
7. Borne at Nicolaud Bridge VEG	62.6	1113	3	20.13	0.95	59.26	-4.21	0.5	0.07	Schists	CM	0.52	1779	0.45
8. Thines at Gournier Bridge VEG	16.73	893	3	16.72	0.81	13.51	-3.51	1.29	0.2	Granite	CS	0.42	1206	0.75
9. Altier at Goulette VEG	103.42	1149	5	17.13	0.94	97.38	-3.71	1.1	0.16	Schists	CLC	0.46	1396	0.55
10. Auzonnet at Mages VEG	49	355	3	14.9	0.36	17.6	-2.39	1.55	0.29	limestones	CM	0.26	978	1.38
11. The Ardèche at Meyras NOVEG	98.43	898	4	23.43	0.96	94.31	-3.74	0.65	-0.2	Granite	CM	0.82	1881	0.15
12. Borne at Nicolaud Bridge NOVEG	62.6	1113	3	20.13	0.95	59.26	-4.08	0.74	-0.15	Schists	CM	0.94	2388	0.09
13. Thines at Gournier Bridge NOVEG	16.73	893	3	16.72	0.81	13.51	-3.71	0.72	-0.13	Granite	CS	0.76	1876	0.12
14. Altier at Goulette NOVEG	103.42	1149	5	17.13	0.94	97.38	-3.8	0.82	-0.02	Schists	CLC	0.86	1417	0.13
15. Auzonnet at Mages NONVEG	49	355	3	14.9	0.36	17.6	-3.31	1.24	-0.26	limestones	CM	0.8	1295	0.34

Table 3- Topographical, meteorological and recession variables used in the FAMD analysis for 5 examined catchments during all years, low-vegetation and vegetation period. Estimated variables are the C_1 , C_2 and C_3 parameters. The other variables are the quantitative and qualitative explanatory variables.

4.1.4 Results of FAMD

The FAMD applied to data set used in this study shows two dimensions that explain about 88% of the variance of the data set (Figure 6). Figure 6 and Table 4 show also the projections of the quantitative variables on these two dimensions and the performance indicators for these projections, respectively. Variables C_1 , C_2 are well correlated to the first dimension, as well as variables PET/P and P_{avg} . It seems like this dimension opposes individuals (catchments) that are more humid / vs dry. Variable C_3 is correlated to the second dimension. Drainage density and altitude seem to be somehow correlated to dimension 2 as well, but this is not so clear. The correlation of qualitative variables can be visualized on factor maps such as Figure 7, where the individuals (catchments) are colored according to their defining qualitative variable (here geology). It can also be observed that catchments cannot be separated according to the land use due to its proximity on the two axes.

However, it can be seen that the groups of catchment are quite separated from one another, and that it is particularly striking for the limestone geology. In addition, geology appears to be the only qualitative variable significantly associated with a dimension. Variance analysis shows that 44% of the variance of the coordinates on dimension 2 is explained by geology.

HCPC according to the principal components reinforces the interpretation of geology being a key parameter. An optimum of four clusters was found. The hierarchical clustering tree of the examined catchments grouped according to their belonging cluster is shown in Figure 8. It can be seen that the clusters mostly follow geological characterization as shown in Figure 7. This is confirmed by a X^2 test, that shows again that geology is the only significant variable linked to the clusters with $p=0.01058961$.

From this analysis, thus it can be concluded that geology is the main driving factor of hydrological variability, and that the recession parameters can be distributed according to the dominant geology in the SIMPLEFLOOD model.

Variable	Correlation		\cos^2	
	Dim 1	Dim 2	Dim 1	Dim 2
C_1	0.86	-0.39	0.73	0.15
C_2	0.87	-0.35	0.76	0.12
C_3	0.37	0.87	0.14	0.76
C	-0.87	-0.38	0.75	0.14
P_{avg}	-0.89	0.20	0.79	0.04
PET/P	0.93	0.18	0.87	0.03
$Area$	-0.14	0.12	0.02	0.01
$Altitude$	-0.61	0.63	0.37	0.40
$Strahler$	-0.04	0.13	0.001	0.02
$Slope$	-0.43	0.40	0.19	0.16
Dd	-0.60	0.64	0.36	0.41
L	-0.30	0.31	0.09	0.09

Table 4- Correlation and \cos^2 values for the examined variables (in red: the variables that are well projected on the first dimension, in blue: the variables that are well projected on the second dimension)

4.2 Model set up

The Ardèche catchment was discretized in sub-catchments with a 10 km² threshold, which is the typical size of convective autumn events and is also consistent with the 8x8 km² resolution of the SAFRAN data. It resulted into 238 modelling units. For each modelling unit, a dominant land use and dominant geology were attributed according to classification presented in Sec 4.1, see Figure 9. The river network was discretized into 238 reaches as well, with average channel length of the sub-catchment being 3.52 km with average channel slope of 3.6 %.

For precipitation input, the weighted average of the overlying SAFRAN cells for each sub-catchment is used. Reference evapotranspiration, ET_0 was calculated from SAFRAN variables using the Penman-Monteith equation. The closest SAFRAN cell to the centroid of sub-catchment was selected. These climate forcings present input in the model (TS input) as shown in Figure 1.

Monthly values for the crop coefficient were determined for each land use according to the FAO database (Allen et al., 1998)). They are used as multiplier to ET_0 as shown in Figure 1. In Table 5, the minimum and maximum values for each land-use type are shown.

ID	Land-use type	K_c min	K_c max
1	Water	1.05	1.05
2	Coniferous Forest	1	1,2
3	Broadleaf Forest	0.74	0.97
4	Mediterranean Forest	1	1.18
5	Urban Areas	1	1
6	Bare Soil	0.3	0.3
7	Early Crops	0.57	1.09
8	Late Crops	0.53	1.14
9	Heath and Shrubs	0.5	1.1

Table 5- Crop coefficient values for respected land-use types

Recession parameters were distributed according to dominant geology as discussed in previous section. They are given in Table 6.

ID	C_1	C_2	C_3
1 (granite)	-3.71	0.72	-0.13
2 (schists)	-3.8	0.82	-0.02
3 (limestone)	-3.31	1.24	-0.26

Table 6- Geology input recession parameters in SIMPLEFLOOD

They were estimated from 5 gauged-catchments from low-vegetation of the 2000-2008 period (Adamovic et al., 2015). Then, the $g(Q)$ function is used for continuous discharge simulation over the 2000-2012 period. In this time series, the high-vegetation periods and 2009-2012 period can be considered as a validation period.

The flow routing scheme implemented in the model assumes simplified rectangular channel bathymetry and thus requires only 4 parameters. Width (b) was set manually according to topographical surveys, rough channel width estimations using Google Earth images, and the Strahler order. The width of the rivers found in the catchment ranged from 1 m to 97 m, with the largest width being on the Ardèche River slightly upstream from the catchment outlet. The roughness coefficient (μ) was set at a uniform value of 30, which is a typical value for natural semi-mountainous streams and corresponds also to the calibrated value obtained with

a 1D hydrodynamic model that was previously set up on the same catchment (Doussiere, 2007). Reach length (l) and slope (α) are product of GIS analysis. The model was run with different initial discharge conditions in order to define the warm-up period. Eventually, year 2000 is chosen as an initial warm-up period and thus was excluded from further evaluation analysis (see Adamovic, 2014).

4.3 Evaluation criteria

To assess model efficiency, Nash-Sutcliffe efficiency and percent bias are used as model evaluation criteria for discharge simulations. Nash-Sutcliffe efficiency, NSE (Nash and Sutcliffe, 1970) is used as a dimensionless model evaluation statistic indicating how well the simulated discharges fit the observations. The NSE as to emphasize the high flows is computed as shown in the following equation:

$$NSE = 1 - \left(\frac{\sum_{i=1}^n (Y_i^{obs} - Y_i^{sim})^2}{\sum_{i=1}^n (Y_i^{obs} - Y^{mean})^2} \right) \quad (4)$$

where Y_i^{obs} is the i -th observation of discharge data, Y_i^{sim} is the simulated discharge value for i -th time step, Y^{mean} is the mean of all observed data and n represents the number of observations.

NSE values range between $-\infty$ and 1.0, with 1 representing the optimal value (see Moriasi et al., 2007, for a recent review of performance criteria). NSE on the logarithm of the discharge is also computed to give less weight to the peaks. For continuous simulation, NSE can be calculated at the hourly time step, because the dam operations influence on peaks can be neglected. However, $\log NSE$ can be calculated only at the daily time step, for which the dis-influenced data could be estimated. While NSE is calculated for continuous and event based simulations, $\log NSE$ is calculated only for continuous simulations.

In addition, percent bias ($PBIAS$) was calculated as a part of the model evaluation statistics. It measures total volume difference between two time series, as Eq. (5) indicates:

$$PBIAS = \frac{\sum_{i=1}^n (Y_i^{sim} - Y_i^{obs}) * 100}{\sum_{i=1}^n (Y_i^{obs})} \quad (5)$$

where Y_i^{obs} is the i^{th} observation of discharge data, Y_i^{sim} is the simulated discharge value for the i^{th} time step, n represents the number of observations and 100 converts the result to percent.

The optimal value of $PBIAS$ is 0.0 where positive values indicate model overestimation bias, and negative values indicate model underestimation bias (e.g. Gupta et al., 1999). Again, in this case, $PBIAS$ can be calculated only at the daily time step for continuous simulation in order to remove the influence of dam operations on observed streamflow.

RMSE represents one of the most used error index statistics (Singh et al., 2004; Vazques-Amabile and Engel, 2005). In the literature usually it is considered that the lower RMSE the better the model performance. The area-weighted root mean square error (NRMSE) is used to determine how closely values match one another while taking into account a normalization factor – area. In that way an adequate comparison across catchments can be provided.

Singh et al. (2004) proposed a so-called RSR model evaluation indicator that is RMSE based on the observations standard deviation in order to better quantify a low RMSE. RSR standardizes RMSE using the observations standard deviation (Moriassi et al., 2007). It is calculated according to the following equation:

$$RSR = \frac{RMSE}{STDEV_{obs}} = \frac{\left[\sqrt{\sum_{i=1}^n (Y_i^{obs} - Y_i^{sim})^2} \right]}{\left[\sqrt{\sum_{i=1}^n (Y_i^{obs} - Y^{mean})^2} \right]} \quad (6)$$

where Y_i^{obs} is the i^{th} observation of discharge data, Y_i^{sim} is the simulated discharge value for i -th time step, Y^{mean} is the mean of all observed data and n represents the number of observations.

RSR includes the benefits of error index statistics along with scaling factor (Moriassi et al., 2007). Optimal value of RSR is 0 which means zero residual variation and good model

simulation whereas positive values indicate not so good modeling performance. RSR is calculated only for continuous based simulations at hourly time step.

5. Results

The SIMPLEFLOOD model was run continuously for the period 2000-2012. Evaluation was performed on a continuous and event-based approach. No parameter calibration was done in the results presented below.

5.1 Continuous simulations

A performance map with NSE calculated at hourly time step is shown on Figure 10. Good efficiencies were obtained for almost all examined catchments except for catchment #3. More precisely, downstream catchments (#10 and #11) showed NSE values of 0.76 and 0.75 respectively.

PBIAS values are also shown in Figure 10 at a daily time step. An underestimation tendency of the discharge is observed for almost all of the examined stations except for catchment #3 where a high overestimation (over 50%) is detected. Using the natural discharge data for influenced stations, PBIAS values become certainly more realistic than if measured discharge had been used, although a general volume underestimation is still observed.

Table 7 gives the complementary information on modeling performance for the catchment outlet (#11). Yearly modeling performance is given separately in addition to the entire simulation period, so that evaluation whether some years are better simulated than others can be done. Year 2002 displays the best simulation in terms of discharge dynamics, with a NSE of 0.75, NSE on log of discharge of 0.78 and the bias compared with naturalized discharge of -15 %, which shows that the simulation underestimated the total volume discharged from the catchment by a certain amount.

Good simulation of discharge dynamics based on high NSE and high NSElog also occurred for the simulations of years 2001, 2003, 2004, 2006, 2008-2012. Although good NSE were seen in these years, similarly to 2002, the model bias for volume discharged was higher. Generally, in all years the model underestimated the discharge. Years when the model performed poorly occurred in 2005 and 2007, with NSE less than 0.28 and a high underestimation of the volume discharged especially in year 2005 (30%). If the RSR is looked at, it can be seen that these years represent dry years with the values approaching almost 1. This is well illustrated in Figure 11 that shows observed and simulated hydrograph for station #1 in year 2005. It can be seen that the model underreacts to all events. This is a common trend seen in our hydrological modelling and could be due to the increased influence of some other processes during dry years such as evapotranspiration, drainage, and groundwater flow, that are not taken into account in the model.

Table 8 shows the summary of modelling performance for all the stations in the Ardèche catchment. According to Moriasi et al. (2007), hydrological simulations can be regarded as “satisfactory” if $NSE > 0.50$, $RSR < 0.70$, and if PBIAS is $\pm 25\%$ for discharge. Table 8 shows that for the majority of stations, satisfactory behavior is obtained except for catchments #4 and #9 where the BIAS was higher/lower than recommended and catchment #3 where NSE, PBIAS and RSR were unsatisfactory. Furthermore, by comparing normalized RMSEs it is noticed that almost all the catchments have the similar values except for catchment #3 where NRMSE was around 0.13.

Year	PBIAS (%)	NSE	NSE_log	RMSE (m ³ /s)	RSR
2001	-1.69	0.72	0.76	44.92	0.53
2002	-3.23	0.85	0.80	52.82	0.39
2003	-18.60	0.82	0.80	78.35	0.42
2004	-5.74	0.74	0.81	61.39	0.51
2005	-30.53	0.23	0.54	43.06	0.88
2006	-21.89	0.66	0.83	65.10	0.58
2007	5.57	0.28	0.44	32.48	0.85

2008	-7.57	0.83	0.88	71.82	0.41
2009	-24.41	0.81	0.73	42.28	0.43
2010	-28.82	0.63	0.84	80.37	0.61
2011	-24.19	0.61	0.84	92.78	0.62
2012	-11.64	0.60	0.70	26.74	0.63
2001-2012	-14.92	0.75	0.78	60.96	0.50

1 Table 7- Modeling performance for the Ardèche at Sauze Saint-Martin (#11) catchment

N°	Station name	NSE	NSElog	PBIAS	NRMSE	RSR
1	<i>Ardèche at Meyras</i>	0.66	0.79	-12	0.05	0.58
2	<i>Borne at Nicoulaud</i>	0.64	0.60	-27	0.07	0.60
3	<i>Thines at Gournier</i>	-1.05	0.65	83	0.13	1.43
4	<i>Altier at Goulette</i>	0.60	-0.96	-40	0.04	0.63
5	<i>Ardèche at Pont-de-Labeaume</i>	0.63	0.46	-15	0.05	0.61
6	<i>Ardèche at Ucel</i>	0.68	-0.10	-29	0.04	0.57
7	<i>Ardèche at Vogue</i>	0.68	0.70	-18	0.04	0.56
8	<i>Baume at Rosieres</i>	0.61	0.53	-32	0.04	0.62
9	<i>Chassezac at Gravieres</i>	0.56	-1.4	105	0.03	0.66
10	<i>Ardèche at Vallon-Pont-d'Arc</i>	0.76	0.65	-13	0.03	0.49
11	<i>Ardèche at Sauze-Saint-Martin</i>	0.75	0.78	-15	0.03	0.50

2 Table 8- Summary of modeling performance in the Ardèche catchment

3 5.2 Event based simulations

4 In this section, discussion about the performance of SIMPLEFLOOD for the event based
5 simulations of 2003, 2008 and 2011 flood events is given.

6 The modeling performance indicators for the examined catchments are given in Table 9.

7 These results are based on hourly averages and not on instantaneous peak discharge values.

8 The catchment behavior varies from event to event giving good NSE and BIAS values for

9 October 2003 and November 2008 event for all catchments except catchment #3 (December

10 2003 event) and catchments #3 and #4 and to a lesser extent catchment #8. For the December

11 2003 event it can be observed that there is around 23 % less water that enters the system

12 (catchment #7) from upstream Ardèche that will eventually be one of the reasons for the

13 hydrograph underestimation at the catchment outlet (Figure 12). These two events occur in wet

14 conditions following significant rainfall in the previous period whereas the October 2008 and

1 November 2011 are associated with dry previous conditions (not shown). These two events
2 show high PBIAS, with a general tendency to underestimate discharge. Figure 12 shows the
3 comparison of simulated and observed hydrograph at the catchment outlet. The November
4 2008 event is best simulated whereas two other events (October 2008 and November 2011)
5 show high discharge underestimation. In addition, Figure 13 gives a comparison of the
6 observed and simulated peak discharge for selected events and examined catchments. The
7 SIMPLEFLOOD model shows overall good performance with R^2 of 0.74, but a tendency to
8 underestimate the highest values, except for the November 2008 event.

		Oct. 2003		Oct. 2008		Nov. 2008		Nov. 2011	
N°	Station name	NSE	PBIAS	NSE	PBIAS	NSE	PBIAS	NSE	PBIAS
1	<i>Ardèche at Meyras</i>	0.56	26	<0.1	1.2	0.64	25	<0.1	-50
2	<i>Borne at Nicoulaud</i>	0.69	6	<0.1	>100	0.86	-15	<0.1	-44
3	<i>Thines at Gournier</i>	<0.1	1.9	<0.1	>100	<0.1	>100	<0.1	-57
4	<i>Altier at Goulette</i>	0.40	-37	<0.1	-82	<0.01	-49	<0.1	-72
5	<i>Ardèche at Pont-de-Labeaume</i>	0.76	-1.5	0.30	49	0.61	7.5	<0.1	-54
6	<i>Ardèche at Ucel</i>	0.83	-12	0.39	-44	0.60	1	<0.1	-52
7	<i>Ardèche at Vogue</i>	0.70	-23	0.24	-54	0.72	6	<0.1	-55
8	<i>Baume at Rosieres</i>	0.63	12	<0.1	>100	0.25	28	<0.1	46
9	<i>Chassezac at Gravieres</i>	0.86	6	0.60	24	0.80	-2	<0.1	-55
10	<i>Ardèche at Vallon-Pont-d'Arc</i>	0.74	-23	0.48	-40	0.94	7.5	0.04	-54
11	<i>Ardèche at Sauze-Saint-Martin</i>	0.65	-29	0.48	-44	0.91	-1	0.05	-59

9 Table 9- Performance indicators at the examined catchments for SIMPLEFLOOD model for
10 2003, 2008 and 2011 flood events.

6. Discussion

In order to construct the SIMPLEFLOOD model several preexisting components from the JAMS repository were used as a part of the model structure (components for creation of modeling units, for input data, climate forcing regionalization and flow routing), which facilitated the model design. Spatial discretization in sub-catchments was done with a size compatible with the catchment heterogeneity and rainfall spatial variability. The discretization of 10 km² appears to be adequate in this case along with use of SAFRAN rainfall data which has a coarse resolution 8x8 km². Other distributed rainfall products are also available on a 1-km² grid (see below). Since high resolution rainfall is recommended in the study of flash floods (Borga et al., 2008), it would be interesting to test the model performance using these rainfall products. Such a study would also require a sensitivity analysis of models' results with regards to catchment discretization in order to see if a finer model discretization is required to really benefit from the 1 km² resolution radar data.

In this study, only the SAFRAN reanalyses are used as rainfall input. The gridded SAFRAN product has been shown to underestimate precipitation especially in mountainous areas and underestimates the occurrence of strong precipitation ($P > 20 \text{ mm day}^{-1}$) (Quintana-Seguí et al., 2008; Vidal et al., 2010). Adamovic et al. (2015) also showed that rainfall correction at the annual scale was required in order to properly close the water balance on some gauged catchments in the Ardèche, and the correction was generally leading to increased rainfall. Rainfall volume underestimation could explain the general discharge underestimation by the model. Some authors tried to overcome the rainfall underestimation problem in mountainous areas by interpolating the SAFRAN data across altitude bands (Etchevers et al., 2001; Lafaysse et al., 2011; Thierion et al., 2012), but these data were not available for the present study. In addition, SAFRAN re-analyses are based on existing rain gauges. In mountainous areas, the few rain gauges that do exist are generally located in lower, flatter terrain, and may

not capture the increase of rainfall with altitude that has been identified in this region (Molinié et al., 2011). It would be interesting to assess the performance of the SIMPLEFLOOD model with other rainfall products inputs. Such study could use the daily rainfall SPAZM reanalysis (Gottardi, 2009) combined with SAFRAN to provide a mixed and more accurate product called DuO (Magand et al., 2014). Delrieu et al. (2014) released a reanalysis merging radar and raingauges data for the 2007-2012 period that can also be used. The impact of rainfall uncertainty can be analyzed using rainfall simulation, in particular using rainfall fields generated using the SAMPO (Leblois and Creutin, 2013) stochastic rainfall generator, conditioned on observations that are also available on the area (Renard et al., 2011). Such analysis, which involves hundreds of simulations, can be facilitated by the simplicity and short computing times of the SIMPLEFLOOD model.

Factor Analysis of Mixed Data (FAMD) was used to identify relationships between discharge sensitivity function parameters and catchment characteristics, including physiographic and hydro-climatic factors. Hierarchical Clustering of Principal Components was also applied in order to clearly identify catchment groups. Dominant geology was found to be the only significant explaining factor. Geology was further used for the regionalization of the SIMPLEFLOOD model parameters. The small sample of catchments could question the robustness of the results. However, the dependence of the model parameters on geology was confirmed on a larger sample of catchments from the Cévennes region in France by Cousot (2015). Vannier et al. (2014) and Garambois et al. (2013) also highlighted geology as a predominant factor that governs the hydrological response in the area. The physical mechanism by which geology governs flash flood response might lie in the hypothesis of shallow subsurface flow caused by saturation of at interface between soil and bedrock. The model results were found sensitive to the way parameters were regionalized according to geology (Adamovic, 2014). Nevertheless, it was possible to select a parameter set providing

satisfactory results on the various gauged catchments, which was further used in the analysis. A more comprehensive analysis of the sensitivity of SIMPLEFLOOD results according to its parameter regionalization would be recommended.

SIMPLEFLOOD results from continuous simulations were found to be satisfactory on the NSE criteria, showing that the model is able to reproduce high discharges satisfactorily, although model performance varies from year to year. A systematic volume underestimation was observed on the simulated discharges, which was reduced on the stations influenced by the Montpezat hydropower plant when “naturalized” discharges were used for their computation. Event based simulations show good modelling performance for two out of four selected flash flood events. Unsatisfactory performance during the October 2008 and November 2011 might be mainly related to the absence of sufficient wetting period before the event. In such contrasted conditions the SIMPLEFLOOD model does not succeed in simulating properly the two chosen events. However, once a certain threshold moisture value is achieved, the model provides good simulations results (e.g. November 2008 event being properly simulated after October 2008 event).

In the simulation performed with SIMPLEFLOOD, it was assumed that $AET = PET = K_C * ET_0$. This probably leads to AET overestimation, which can contribute also to underestimated discharge simulation, especially in summer when vegetation is active. As expected from the results of Adamovic et al. (2015), the model was found to have better performance in winter and wet periods than in summer when evapotranspiration plays an important role. Nevertheless, evapotranspiration is not the dominant process during flash floods and the approximation used to compute AET can be considered as satisfactory for those periods. The model is generally not able to simulate properly the first events in the autumn season. This could be related to the overestimation of AET in summer that could lead to a too large decrease of catchment storage.

In Adamovic et al. (2015), numerous perspectives and limitations are given. The sampling strategy of deriving the $g(Q)$ function from low-vegetation periods appeared to be adequate in our case. The results show that the information retrieved from only a function of the discharge time series is relevant also for periods with very different characteristics. We believe that the approach could be applied in other catchments as well once the soil moisture threshold is reached. The approach performs better during the wet, winter periods than the dry, summer periods probably due to the still not yet fully adaptability to the high evapotranspiration conditions that exist in Mediterranean catchments. However, the approach could derive better results in those regions where *ETP* presents a small fraction of the water balance equation. We argue that testing this approach on new data sets, for various climatic conditions, contributes to the advance of hydrological science itself. The major limitation of the SDSA is of course the availability of good quality discharge data with a short time step, in catchments representative of the spatial variability of hydro-climatic conditions. Discharge must also be representative of natural conditions, which could also limit its applicability in catchments impacted by human activity. The approach cannot also be applied in regions where Hortonian overland flow is dominant, unless certain bypass mechanism is introduced (Kirchner, 2009). It cannot be neither applied to ephemeral streams because if discharge is zero, storage will have the same value and thus $g(Q)$ function will be ill defined.

7. Conclusions

In Adamovic et al. (2015), it was showed how the simple dynamical system top-down approach, applied to gauged catchments, provides knowledge of dominant hydrological processes in the specific context of Mediterranean catchments. The model parameters were estimated using recession analysis and used for continuous simulations. In this study, this

approach was successfully extended to build a distributed hydrological model, called SIMPLEFLOOD, at the regional scale (2300 km²). Model parameters were regionalized based on dominant geology. The model was continuously applied with an hourly time step in the Ardèche catchment for the 2000-2012 period, that includes several flash flood events. Model results were satisfactory over the whole period, with a large annual variability of criteria, and a general tendency to have worse performance during dry years. Good model performance was also achieved for flash flood events occurring in wet conditions, whereas the model failed to simulate the volume of events occurring after a dry period. This is consistent with Adamovic et al. (2015) who showed that rapid sub-surface flow which is a process included in the simple dynamical system approach is dominant in wet conditions. On the other hand, the model should be improved to achieve good performance under dry conditions, in particular in terms of actual evapotranspiration representation.

Further evaluation on other catchments is recommendable to better understand under which conditions this type of model is applicable. Sensitivity to catchment discretization and rainfall resolution and uncertainty should also be performed.

Acknowledgments

The study is conducted within the FloodScale project, funded by the French National Research Agency (ANR) under contract n° ANR 2011 BS56 027, which contributes to the HyMeX program. The HyMeX database teams (ESPRI/IPSL and SEDOO/Observatoire Midi-Pyrénées) helped in accessing the data. The authors acknowledge Brice Boudevillain for providing the OHM-CV rainfall data, Météo-France for their rainfall and SAFRAN climate data. EdF-DTG provided discharge data from three of the gauges used in this study. Julien

Andrieu is thanked for providing the landuse map used in the study. We thank the Region Rhône-Alpes for its funding of the PhD grant of the first author.

References

- Adamovic, M., 2014. Development of a data-driven distributed hydrological model for regional catchments prone to Mediterranean flash floods. Application to the Ardèche catchment (France). PhD thesis, University of Grenoble, France, 326.
- Adamovic, M., Braud, I., Branger, F., and Kirchner, J. W., 2015. Assessing the simple dynamical systems approach in a Mediterranean context: application to the Ardèche catchment (France), *Hydrol. Earth Syst. Sci.*, 19, 2427-2449, doi:10.5194/hess-19-2427-2015.
- Allen, R., Pereira, L., Raes, D., and Smith, M., 1998. Crop evapotranspiration - Guidelines for computing crop water requirements - FAO Irrigation and drainage paper 56, citeulike-article-id:10458368.
- Anquetin, S., Braud, I., Vannier, O., Viallet, P., Boudevillain, B., Creutin, J.-D., and Manus, C., 2010. Sensitivity of the hydrological response to the variability of rainfall fields and soils for the Gard 2002 flash-flood event, *Journal of Hydrology*, 394, 134-147, <http://dx.doi.org/10.1016/j.jhydrol.2010.07.002>.
- Bathurst, J.C., Burton, A., Clarke, B.G., and Gallart, F. 2006. Application of the SHETRAN basin-scale, landslide sediment yield model to the Llobregat basin, Spanish Pyrenees. *Hydrol. Process.*, 20, 3119-3138.
- Beven, K., 2012. *Rainfall-runoff Modelling – The Primer*, Wiley: Chichester.
- Bloschl, G., and Sivapalan, M., 1995. Scale issues in hydrological modelling: a review, *Hydrological Processes*, 9, 251-290.
- Bonnifait, L., Delrieu, G., Lay, M. L., Boudevillain, B., Masson, A., Belleudy, P., Gaume, E., and Saulnier, G.-M., 2009. Distributed hydrologic and hydraulic modelling with radar rainfall input: Reconstruction of the 8–9 September 2002 catastrophic flood event in the Gard region, France, *Advances in Water Resources*, 32, 1077-1089, <http://dx.doi.org/10.1016/j.advwatres.2009.03.007>.
- Borga, M., and Morin, E., 2014. Characteristics of Flash Flood Regimes in the Mediterranean Region, in: *Storminess and Environmental Change*, edited by: Diodato, N., and Bellocchi, G., Springer, *Advances in Natural and Technological Hazards Research*, Netherlands, 65-76.

- 1 Borgia, M., Gaume, E., Creutin, J. D., and Marchi, L., 2008. Surveying flash floods: gauging
2 the ungauged extremes, *Hydrological Processes*, 22, 3883-3885, 10.1002/hyp.7111.
- 3
- 4 Boudevillain, B., Delrieu, G., Galabertier, B., Bonnifait, L., Bouilloud, L., Kirstetter, P.-E.,
5 and Mosini, M.-L., 2011. The Cévennes-Vivarais Mediterranean Hydrometeorological
6 Observatory database, *Water Resources Research*, 47, W07701, 10.1029/2010wr010353.
- 7
- 8 Braud, I., Ayral, P. A., Bouvier, C., Branger, F., Delrieu, G., Le Coz, J., Nord, G.,
9 Vandervaere, J. P., Anquetin, S., Adamovic, M., Andrieu, J., Batiot, C., Boudevillain, B.,
10 Brunet, P., Carreau, J., Confoland, A., Didon-Lescot, J. F., Domergue, J. M., Douvinet, J.,
11 Dramais, G., Freydier, R., Gérard, S., Huza, J., Leblois, E., Le Bourgeois, O., Le Boursicaud,
12 R., Marchand, P., Martin, P., Nottale, L., Patris, N., Renard, B., Seidel, J. L., Taupin, J. D.,
13 Vannier, O., Vincendon, B., and Wijbrans, A., 2014. Multi-scale hydrometeorological
14 observation and modelling for flash-flood understanding, *Hydrol. Earth Syst. Sci.* 11, 1871-
15 1945, 10.5194/hessd-11-1871-2014.
- 16
- 17 Braud, I., Roux, H., Anquetin, S., Maubourguet, M.-M., Manus, C., Viallet, P., and Dartus,
18 D., 2010. The use of distributed hydrological models for the Gard 2002 flash flood event:
19 Analysis of associated hydrological processes, *Journal of Hydrology*, 394, 162-181,
20 <http://dx.doi.org/10.1016/j.jhydrol.2010.03.033>.
- 21
- 22 Brauer, C. C., Teuling, A. J., Torfs, P. J. J. F., and Uijlenhoet, R., 2013. Investigating storage-
23 discharge relations in a lowland catchment using hydrograph fitting, recession analysis, and
24 soil moisture data, *Water Resources Research*, 49, 4257-4264, 10.1002/wrcr.20320.
- 25
- 26 Coopersmith, E., Yaeger, M. A., Ye, S., Cheng, L., and Sivapalan, M., 2012. Exploring the
27 physical controls of regional patterns of flow duration curves – Part 3: A catchment
28 classification system based on regime curve indicators, *Hydrol. Earth Syst. Sci.*, 16, 4467-
29 4482, 10.5194/hess-16-4467-2012.
- 30
- 31 Coussot, C., 2015. Assessing and modelling hydrological behaviours of Mediterranean
32 catchments using discharge recession analysis. Master Thesis, HydroHazards, University of
33 Grenoble, France, 54 pp.
- 34
- 35 Delrieu, G., Wijbrans, A., Boudevillain, B., Faure, D., Bonnifait, L., and Kirstetter, P.-E.,
36 2014. Geostatistical radar–raingauge merging: A novel method for the quantification of rain
37 estimation accuracy, *Advances in Water Resources*, 71, 110-124,
38 <http://dx.doi.org/10.1016/j.advwatres.2014.06.005>.
- 39
- 40 Di Prinzio, M., Castellarin, A., and Toth, E., 2011. Data-driven catchment classification:
41 application to the pub problem, *Hydrol. Earth Syst. Sci.*, 15, 1921-1935, 10.5194/hess-15-
42 1921-2011.
- 43

- 1 Drobinski, P., Ducrocq, V., Alpert, P., Anagnostou, E., Béranger, K., Borga, M., Braud, I.,
2 Chanzy, A., Davolio, S., Delrieu, G., Estournel, C., Boubrahmi, N. F., Font, J., Grubisic, V.,
3 Gualdi, S., Homar, V., Ivancan-Picek, B., Kottmeier, C., Kotroni, V., Lagouvardos, K.,
4 Lionello, P., Llasat, M. C., Ludwig, W., Lutoff, C., Mariotti, A., Richard, E., Romero, R.,
5 Rotunno, R., Roussot, O., Ruin, I., Somot, S., Taupier-Letage, I., Tintore, J., Uijlenhoet, R.,
6 and Wernli, H., 2013. HyMeX, a 10-year multidisciplinary program on the Mediterranean
7 water cycle, Bulletin of the American Meteorological Society, 10.1175/BAMS-D-12-00242.1.
8
- 9 Etchevers, P., Durand, Y., Habets, F., Martin, E., and Noilhan, J., 2001. Impact of spatial
10 resolution on the hydrological simulation of the Durance high-Alpine catchment, France,
11 Annals of Glaciology, 32, 87-92.
12
- 13 Fink, M., Krause, P., Kralisch, S., Bende-Michl, U., and Flügel, W. A., 2007. Development
14 and application of the modelling system J2000-S for the EU-water framework directive, Adv.
15 Geosci., 11, 123-130, 10.5194/adgeo-11-123-2007.
16
- 17 Flügel, W.-A., 1995. Delineating hydrological response units by geographical information
18 system analyses for regional hydrological modelling using PRMS/MMS in the drainage basin
19 of the River Bröl, Germany, Hydrological Processes, 9, 423-436, 10.1002/hyp.3360090313.
20
- 21 Frattini, P., Crosta, G. and Sosio, R. 2009. Approaches for defining thresholds and return
22 periods for rainfall-triggered shallow landslides. Hydrol. Process., 23, 1444-1460.
23
- 24 Freeze, R. A., and Harlan, R. L., 1969. Blueprint for a physically-based, digitally-simulated
25 hydrologic response model, Journal of Hydrology, 9, 237-258,
26 [http://dx.doi.org/10.1016/0022-1694\(69\)90020-1](http://dx.doi.org/10.1016/0022-1694(69)90020-1).
27
- 28 Garambois, P. A., Roux, H., Larnier, K., Castaings, W., and Dartus, D., 2013.
29 Characterization of process-oriented hydrologic model behavior with temporal sensitivity
30 analysis for flash floods in Mediterranean catchments, Hydrol. Earth Syst. Sci., 17, 2305-
31 2322, 10.5194/hess-17-2305-2013.
32
- 33 Gaume, E., Bain, V., Bernardara, P., Newinger, O., Barbuc, M., Bateman, A., Blaškovičová,
34 L., Blöschl, G., Borga, M., Dumitrescu, A., Daliakopoulos, I., Garcia, J., Irimescu, A.,
35 Kohnova, S., Koutroulis, A., Marchi, L., Matreata, S., Medina, V., Preciso, E., Sempere-
36 Torres, D., Stancalie, G., Szolgay, J., Tsanis, I., Velasco, D., and Viglione, A., 2009. A
37 compilation of data on European flash floods, Journal of Hydrology, 367, 70-78,
38 <http://dx.doi.org/10.1016/j.jhydrol.2008.12.028>.
39
- 40 Gaume, E., Livet, M., Desbordes, M., and Villeneuve, J. P., 2004. Hydrological analysis of
41 the river Aude, France, flash flood on 12 and 13 November 1999, Journal of Hydrology, 286,
42 135-154, <http://dx.doi.org/10.1016/j.jhydrol.2003.09.015>.
43

- 1 Giorgi, F., 2006. Climate change hot-spots, *Geophysical Research Letters*, 33, L08707,
2 10.1029/2006GL025734.
- 3
- 4 Gottardi, F., 2009. Estimation statistique et reanalyse des precipitations en montagne -
5 Utilisation d'ébauches par types de temps et assimilation de donnees d'enneigement :
6 Application aux grands massifs montagneux francais, *Hydrology*, Institut Polytechnique de
7 Grenoble-INPG, French, <https://tel.archives-ouvertes.fr/>, 261 pp.
- 8
- 9 Gourley, J.J., Flamig, Z.L., Hong, Y., Howard, K.W., 2014. Evaluation of past, present and
10 future tools for radar-based flash-flood prediction in the USA. *Hydrological Sciences Journal*,
11 59(7): 1377-1389.
- 12
- 13 Gupta, H. V., Sorooshian, S., and Yapo, P. O., 1999. Status of automatic calibration for
14 hydrologic models: Comparison with multilevel expert calibration, *Journal of Hydrologic*
15 *Engineering*, 4, 135-143.
- 16
- 17 Hapuarachchi, H. A. P., Wang, Q. J., and Pagano, T. C., 2011. A review of advances in flash
18 flood forecasting, *Hydrological Processes*, 25, 2771-2784, 10.1002/hyp.8040.
- 19
- 20 He, Y., Bárdossy, A., and Zehe, E., 2011. A catchment classification scheme using local
21 variance reduction method, *Journal of Hydrology*, 411, 140-154,
22 <http://dx.doi.org/10.1016/j.jhydrol.2011.09.042>.
- 23
- 24 Herbst, M., Gupta, H. V., and Casper, M. C., 2008. Mapping model behaviour using Self-
25 Organizing Maps, *Hydrol. Earth Syst. Sci. Discuss.*, 5, 3517-3555, 10.5194/hessd-5-3517-
26 2008.
- 27
- 28 Kirchner, J. W., 2009. Catchments as simple dynamical systems: Catchment characterization,
29 rainfall-runoff modeling, and doing hydrology backward, *Water Resources Research*, 45,
30 W02429, 10.1029/2008WR006912.
- 31
- 32 Kirchner, J. W., 2006. Getting the right answers for the right reasons: Linking measurements,
33 analyses, and models to advance the science of hydrology, *Water Resources Research*, 42,
34 W03S04, 10.1029/2005wr004362.
- 35
- 36 Klemeš, V., 1983. Conceptualization and scale in hydrology, *Journal of Hydrology*, 65, 1-23,
37 [http://dx.doi.org/10.1016/0022-1694\(83\)90208-1](http://dx.doi.org/10.1016/0022-1694(83)90208-1).
- 38
- 39 Kralisch, S., and Krause, P., 2006. JAMS - A Framework for Natural Resource Model
40 Development and Application, iEMSs Third Biannual Meeting "Summit on Environmental
41 Modelling and Software", Burlington, USA.
- 42

- 1 Krause, P., and Hanisch, S., 2009. Simulation and analysis of the impact of projected climate
2 change on the spatially distributed water balance in Thuringia, Germany, *Adv. Geosci.*, 21,
3 33-48, 10.5194/adgeo-21-33-2009.
- 4
- 5 Krause, P., Bäse, F., Bende-Michl, U., Fink, M., Flügel, W., and Pfennig, B., 2006.
6 Multiscale investigations in a mesoscale catchment-hydrological modelling in the Gera
7 catchment, *Adv. Geosci.*, 9, 53-61, 10.5194/adgeo-9-53-2006.
- 8
- 9 Lafaysse, M., Hingray, B., Etchevers, P., Martin, E., and Obled, C., 2011. Influence of spatial
10 discretization, underground water storage and glacier melt on a physically-based hydrological
11 model of the Upper Durance River basin, *Journal of Hydrology*, 403, 116-129.
- 12
- 13 Lang, M., Moussay, D., Recking, A., and Naulet, R., 2002. Hydraulic modelling of historical
14 floods: a case study on the Ardeche river at Vallon-Pont-d'Arc, 183-189.
- 15
- 16 Le, S., Josse, J., and Husson, F.: FactoMineR, 2008. An R package for multivariate analysis,
17 *Journal of statistical software*, 25, 1-18.
- 18
- 19 Leblois, E., and Creutin, J.-D., 2013. Space-time simulation of intermittent rainfall with
20 prescribed advection field: Adaptation of the turning band method, *Water Resources*
21 *Research*, 49, 3375-3387, 10.1002/wrcr.20190.
- 22
- 23 Ley, R., Casper, M. C., Hellebrand, H., and Merz, R., 2011. Catchment classification by
24 runoff behaviour with self-organizing maps (SOM), *Hydrol. Earth Syst. Sci.*, 15, 2947-2962,
25 10.5194/hess-15-2947-2011.
- 26
- 27 Magand, C., Ducharne, A., Le Moine, N., and Gascoin, S., 2014. Introducing Hysteresis in
28 Snow Depletion Curves to Improve the Water Budget of a Land Surface Model in an Alpine
29 Catchment, *Journal of Hydrometeorology*, 15, 631-649, 10.1175/JHM-D-13-091.1.
- 30
- 31 Manus, C., Anquetin, S., Braud, I., Vandervaere, J. P., Creutin, J. D., Viallet, P., and Gaume,
32 E., 2009. A modeling approach to assess the hydrological response of small mediterranean
33 catchments to the variability of soil characteristics in a context of extreme events, *Hydrol.*
34 *Earth Syst. Sci.*, 13, 79-97, 10.5194/hess-13-79-2009.
- 35
- 36 McDonnell, J. J., and Woods, R., 2004. On the need for catchment classification, *Journal of*
37 *Hydrology*, 299, 2-3, <http://dx.doi.org/10.1016/j.jhydrol.2004.09.003>.
- 38
- 39 Melsen, L. A., Teuling, A. J., van Berkum, S. W., Torfs, P. J. J. F., and Uijlenhoet, R., 2014.
40 Catchments as simple dynamical systems: A case study on methods and data requirements for
41 parameter identification, *Water Resources Research*, 50, 5577-5596,
42 10.1002/2013WR014720.
- 43

- 1 Molinié, G., Ceresetti, D., Anquetin, S., Creutin, J. D., and Boudevillain, B., 2011. Rainfall
2 Regime of a Mountainous Mediterranean Region: Statistical Analysis at Short Time Steps,
3 Journal of Applied Meteorology and Climatology, 51, 429-448, 10.1175/2011JAMC2691.1.
4
- 5 Moriasi, D. N., Arnold, J. G., Van Liew, M. W., Bingner, R. L., Harmel, R. D., and Veith, T.
6 L., 2007. Model evaluation guidelines for systematic quantification of accuracy in watershed
7 simulations, Transactions of the ASABE, 50, 885-900.
8
- 9 Nash, J. E., and Sutcliffe, J. V., 1970. River flow forecasting through conceptual models part I
10 - A discussion of principles, Journal of Hydrology, 10, 282-290.
11
- 12 Naulet, R., Lang, M., Ouarda, T. B. M. J., Coeur, D., Bobée, B., Recking, A., and Moussay,
13 D., 2005. Flood frequency analysis on the Ardèche river using French documentary sources
14 from the last two centuries, Journal of Hydrology, 313, 58-78.
15
- 16 Noël, J.-F., 2014. Naturalisation de debits observes sur le bassin versant de l'Ardeche Irstea
17 and ENTPE, Master thesis, 74.
18
- 19 Pagès, J., 2004. Analyse factorielle de données mixtes, Revue de Statistique Appliquée 93-
20 111.
21
- 22 Quintana-Seguí, P., Le Moigne, P., Durand, Y., Martin, E., Habets, F., Baillon, M., Canellas,
23 C., Franchisteguy, L., and Morel, S., 2008. Analysis of near-surface atmospheric variables:
24 Validation of the SAFRAN analysis over France, Journal of Applied Meteorology and
25 Climatology, 47, 92-107.
26
- 27 Reager, J. T., Famiglietti, J. S., 2009. Global terrestrial water storage capacity and flood
28 potential using GRACE, Geophys. Res. Lett., 36, L23402, [doi:10.1029/2009GL040826](https://doi.org/10.1029/2009GL040826).
29
- 30 Renard, B. et al., 2011. Quantifying uncertainties in hydrologic prediction, with application to
31 flood forecasting, FAST Project 23126WL report, 48 pp.
32
- 33 Roux, H., Labat, D., Garambois, P. A., Maubourguet, M. M., Chorda, J., and Dartus, D.,
34 2011. A physically-based parsimonious hydrological model for flash floods in Mediterranean
35 catchments, Nat. Hazards Earth Syst. Sci., 11, 2567-2582, 10.5194/nhess-11-2567-2011.
36
- 37 Rozalis, S., Morin, E., Yair, Y., Price, C., 2010. Flash flood prediction using an uncalibrated
38 hydrological model and radar rainfall data in a Mediterranean watershed under changing
39 hydrological conditions. Journal of Hydrology, 394(1-2): 245-255.
40
- 41 Samaniego, L., Kumar, R., and Attinger, S., 2010. Multiscale parameter regionalization of a
42 grid-based hydrologic model at the mesoscale, Water Resources Research, 46, W05523,
43 10.1029/2008WR007327.

- 1
- 2 Sangati, M., and Borga, M., 2009. Influence of rainfall spatial resolution on flash flood
- 3 modelling, *Nat. Hazards Earth Syst. Sci.*, 9, 575-584, 10.5194/nhess-9-575-2009.
- 4
- 5 Saulnier, G. M., and Le Lay, M., 2009. Sensitivity of flash-flood simulations on the volume,
- 6 the intensity, and the localization of rainfall in the Cévennes-Vivarais region (France), *Water*
- 7 *Resources Research*, 45, W10425, 10.1029/2008WR006906.
- 8
- 9 Sawicz, K., Wagener, T., Sivapalan, M., Troch, P. A., and Carrillo, G., 2011. Catchment
- 10 classification: empirical analysis of hydrologic similarity based on catchment function in the
- 11 eastern USA, *Hydrol. Earth Syst. Sci.*, 15, 2895-2911, 10.5194/hess-15-2895-2011.
- 12
- 13 Silvestro, F., Gabellani, S., Delogu, F., Rudari, R., Boni, G., 2013. Exploiting remote sensing
- 14 land surface temperature in distributed hydrological modelling: the example of the Continuum
- 15 model. *Hydrol. Earth Syst. Sci.*, 17, 39-62, 2013. doi:10.5194/hess-17-39-2013.
- 16
- 17 Silvestro, F., Rebora, N. and Ferraris, L., 2011. Quantitative flood forecasting on small and
- 18 medium size basins: a probabilistic approach for operational purposes. *Journal of*
- 19 *Hydrometeorology*, 12(6), 1432-1446.
- 20 Singh, J., Knapp, H. V., and Demissie, M., 2004. Hydrologic modeling of the Iroquois River
- 21 watershed using HSPF and SWAT, ISWS CR 2004-08. Champaign, Ill.: Illinois State Water
- 22 Survey.
- 23
- 24 Sivapalan, M., 2003a. Process complexity at hillslope scale, process simplicity at the
- 25 watershed scale: is there a connection?, *Hydrological Processes*, 17, 1037-1041,
- 26 10.1002/hyp.5109.
- 27
- 28 Sivapalan, M., 2003b. Prediction in ungauged basins: a grand challenge for theoretical
- 29 hydrology, *Hydrological Processes*, 17, 3163-3170, 10.1002/hyp.5155.
- 30
- 31 Tarboton, D. G., 1997. A new method for the determination of flow directions and upslope
- 32 areas in grid digital elevation models, *Water Resources Research*, 33, 309-319,
- 33 10.1029/96WR03137.
- 34 Teuling, A. J., Lehner, I., Kirchner, J. W., and Seneviratne, S. I., 2010. Catchments as simple
- 35 dynamical systems: Experience from a Swiss prealpine catchment, *Water Resources*
- 36 *Research*, 46, W10502, 10.1029/2009WR008777.
- 37
- 38 Thierion, C., Longuevergne, L., Habets, F., Ledoux, E., Ackerer, P., Majdalani, S., Leblois,
- 39 E., Lecluse, S., Martin, E., Queguiner, S., and Viennot, P., 2012. Assessing the water balance
- 40 of the Upper Rhine Graben hydrosystem, *Journal of Hydrology*, 424–425, 68-83,
- 41 <http://dx.doi.org/10.1016/j.jhydrol.2011.12.028>.
- 42

- 1 Toth, E., 2013. Catchment classification based on characterisation of streamflow and
2 precipitation time series, *Hydrol. Earth Syst. Sci.*, 17, 1149-1159, 10.5194/hess-17-1149-
3 2013.
- 4
- 5 Tramblay Y., Bouvier C., Crespy A., Marchandise A., 2010. Improvement of flash flood
6 modelling using spatial patterns of rainfall: a case study in south of France. *Global Change:*
7 *Facing Risks and Threats to Water Resources* (Proceedings of the Sixth World FRIEND
8 Conference, Fez, Morocco, October 2010). IAHS Publ. 340, 172-178,
9 <http://y.tramblay.free.fr/doc/Tramblay-redbook.340.pdf>.
- 10
- 11 Vannier, O., Braud, I., and Anquetin, S., 2014. Regional estimation of catchment-scale soil
12 properties by means of streamflow recession analysis for use in distributed hydrological
13 models, *Hydrological Processes*, 28, 6276-6291, 10.1002/hyp.10101.
- 14
- 15 Vannier, O., 2013. Apport de la modélisation hydrologique régionale à la compréhension des
16 processus de crue en zone méditerranéenne, Thèse de l'Ecole doctorale Terre, Univers,
17 Environnement, University of Grenoble, Grenoble, France, 22 Novembre 2013, 274 pp.
- 18
- 19 Vazques-Amabile, G. G., and Engel, B. A., 2005. Use of swat to compute groundwater table
20 depth and streamflow in the muscatatuck river watershed, 3, *American Society of Agricultural*
21 *Engineers*, St. Joseph, MI, ETATS-UNIS, 13 pp.
- 22
- 23 Vidal, J. P., Martin, E., Franchistéguy, L., Baillon, M., and Soubeyroux, J. M., 2010. A 50-
24 year high-resolution atmospheric reanalysis over France with the Safran system, *International*
25 *Journal of Climatology*, 30, 1627-1644.
- 26
- 27 Vincendon, B., Ducrocq, V., Saulnier, G.-M., Bouilloud, L., Chancibault, K., Habets, F., and
28 Noilhan, J., 2010. Benefit of coupling the ISBA land surface model with a TOPMODEL
29 hydrological model version dedicated to Mediterranean flash-floods, *Journal of Hydrology*,
30 394, 256-266, <http://dx.doi.org/10.1016/j.jhydrol.2010.04.012>.
- 31
- 32 Wagener, T., Sivapalan, M., Troch, P., and Woods, R., 2007. Catchment Classification and
33 Hydrologic Similarity, *Geography Compass*, 1, 901-931, 10.1111/j.1749-8198.2007.00039.x.
- 34
- 35 Winter, T. C., 2001. The concept of hydrologic landscapes, *JAWRA Journal of the American*
36 *Water Resources Association*, 37, 335-349, 10.1111/j.1752-1688.2001.tb00973.x.
- 37
- 38 Yaeger, M., Coopersmith, E., Ye, S., Cheng, L., Viglione, A., and Sivapalan, M., 2012.
39 Exploring the physical controls of regional patterns of flow duration curves; Part 4: A
40 synthesis of empirical analysis, process modeling and catchment classification, *Hydrol. Earth*
41 *Syst. Sci.*, 16, 4483-4498, 10.5194/hess-16-4483-2012.

1 Zanon, F., Borga, M., Zoccatelli, D., Marchi, L., Gaume, E., Bonnifait, L., Delrieu, G., 2010.
2 Hydrological analysis of a flash flood across a climatic and geologic gradient The September
3 18, 2007 event in Western Slovenia. *Journal of Hydrology*, 394(1-2): 182-197.

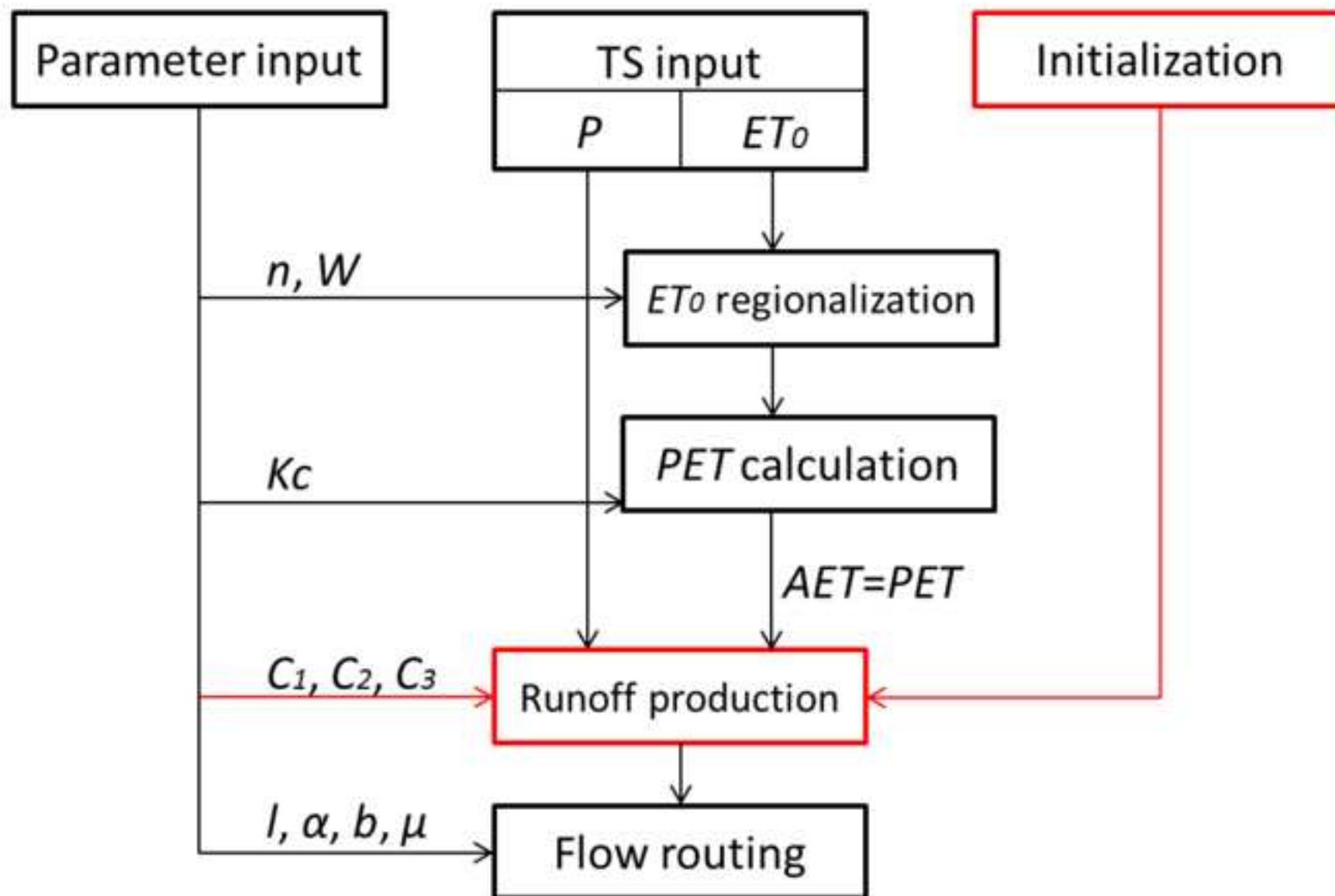
4
5 Zehe, E., Lee, H., and Sivapalan, M., 2006. Dynamical process upscaling for deriving
6 catchment scale state variables and constitutive relations for meso-scale process models,
7 *Hydrology and Earth System Sciences*, 10, 981-996.

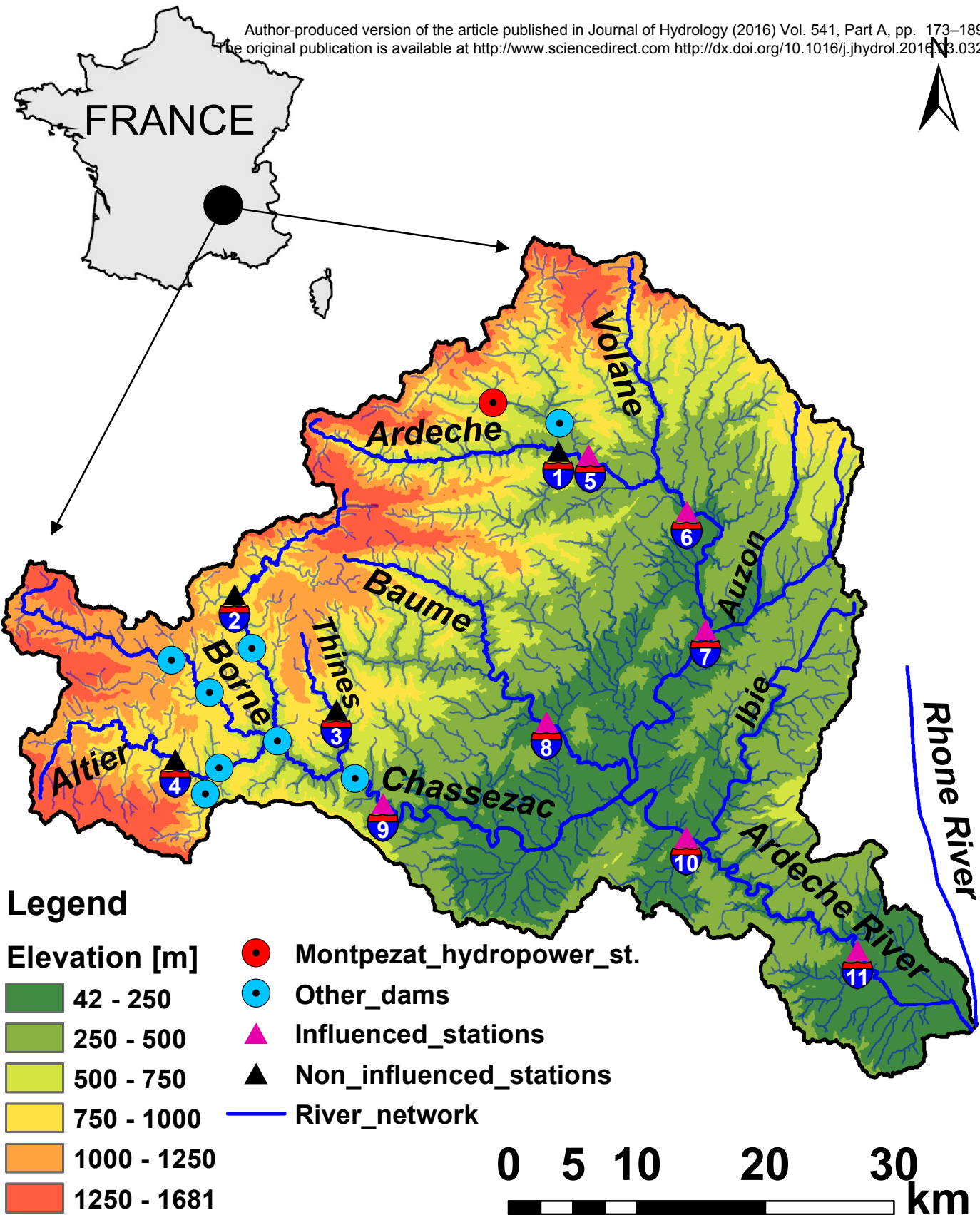
8
9 Zoccatelli, D., Borga, M., Zanon, F., Antonescu, B., Stancalie, G., 2010. Which rainfall
10 spatial information for flash flood response modelling? A numerical investigation based on
11 data from the Carpathian range, Romania. *Journal of Hydrology*, 394(1-2): 148-161.

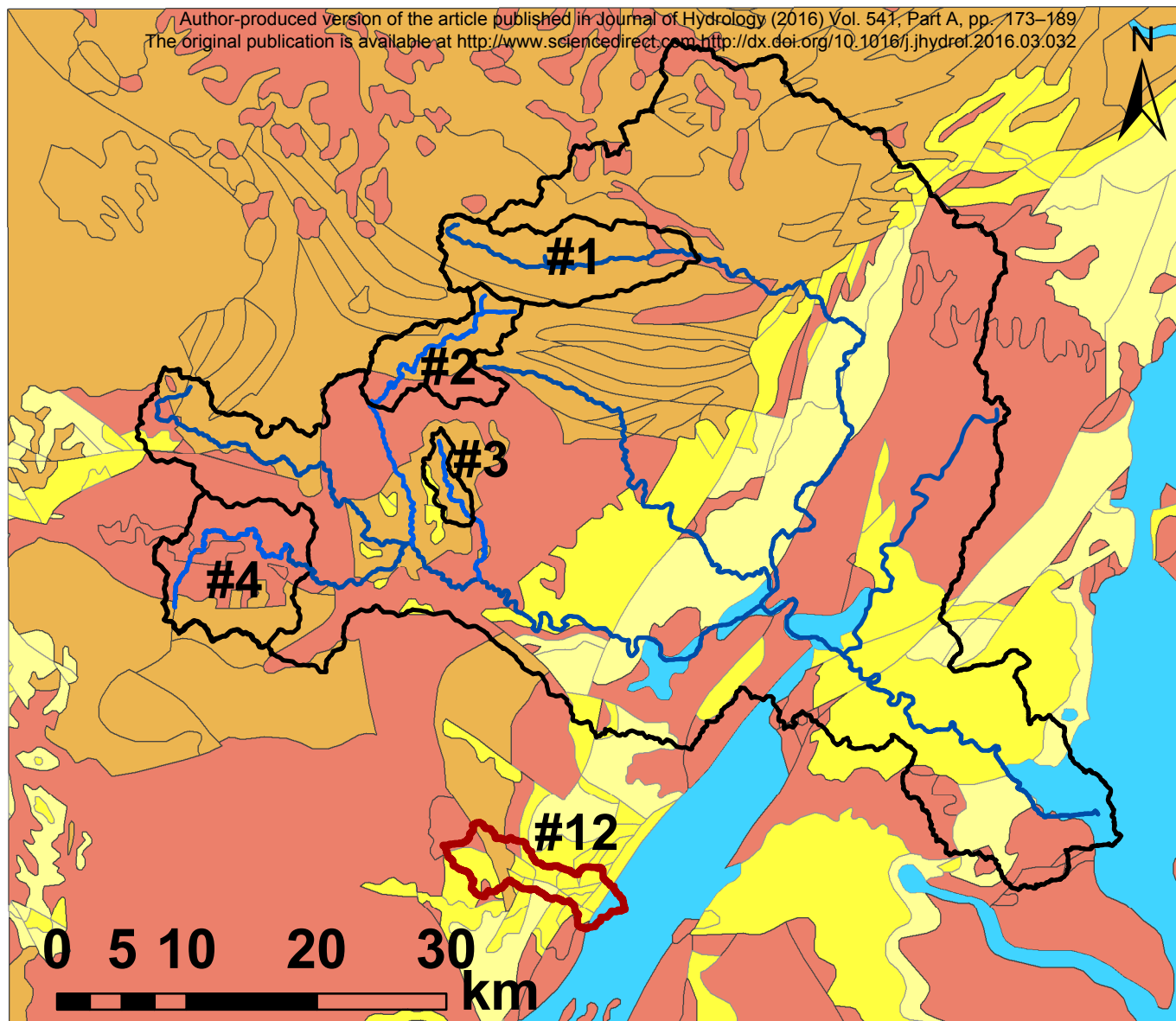
Figure 1

[Click here to download high resolution image](#)

Author-produced version of the article published in Journal of Hydrology (2016) Vol. 541, Part A, pp. 173–189
The original publication is available at <http://www.sciencedirect.com> <http://dx.doi.org/10.1016/j.jhydrol.2016.03.032>







Geology

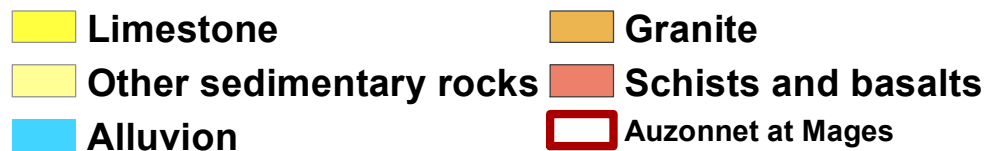


Figure 4

[Click here to download high resolution image](#)

Author's personal version of the article published in Journal of Hydrology (2016) Vol. 541, Part A, pp. 173–189
The original publication is available at <http://www.sciencedirect.com> <http://dx.doi.org/10.1016/j.jhydrol.2016.03.032>

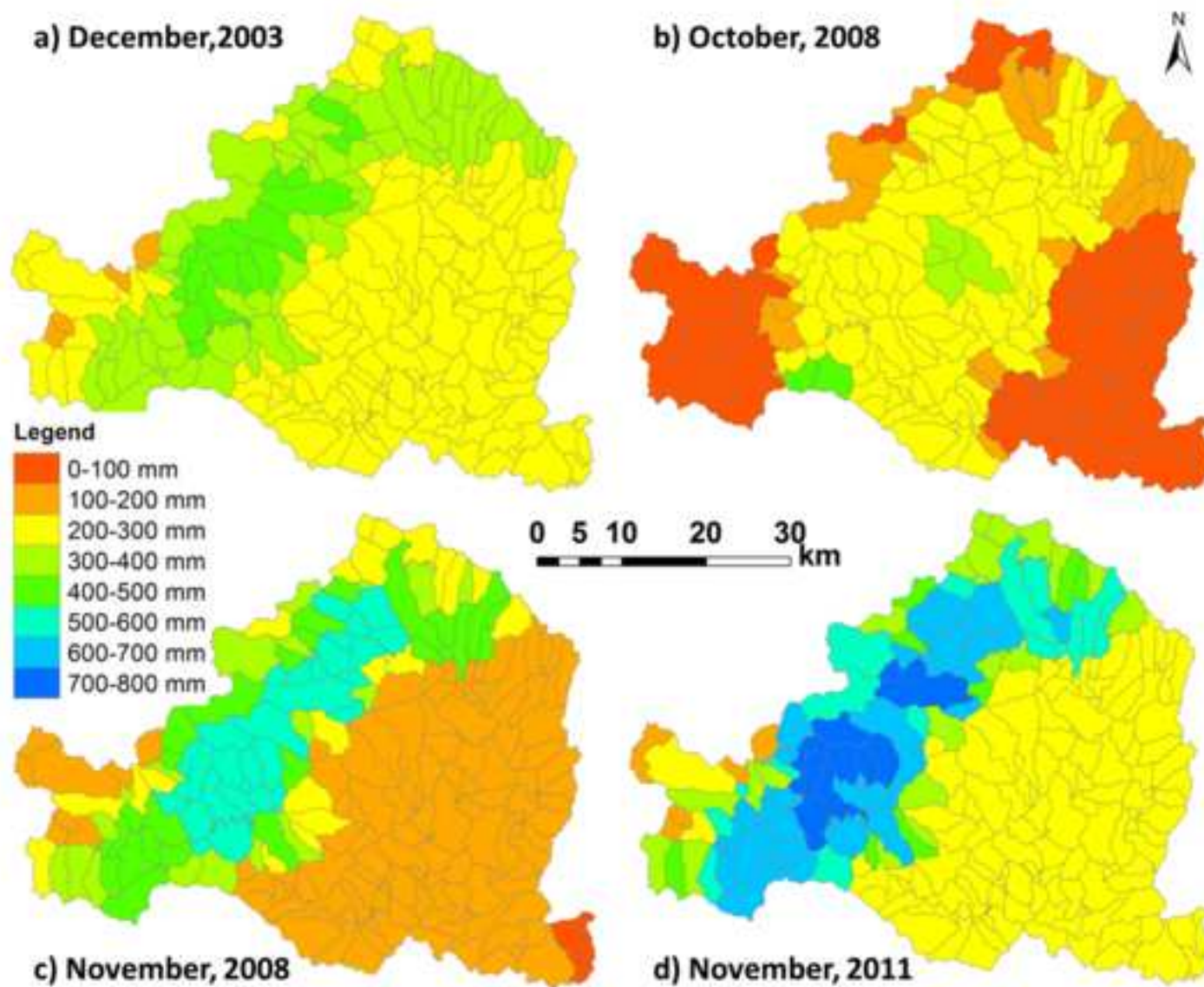


Figure 5

Author-produced version of the article published in Journal of Hydrology (2016) Vol. 541, Part A, pp. 173–189
The original publication is available at <http://www.sciencedirect.com> <http://dx.doi.org/10.1016/j.jhydrol.2016.03.032>

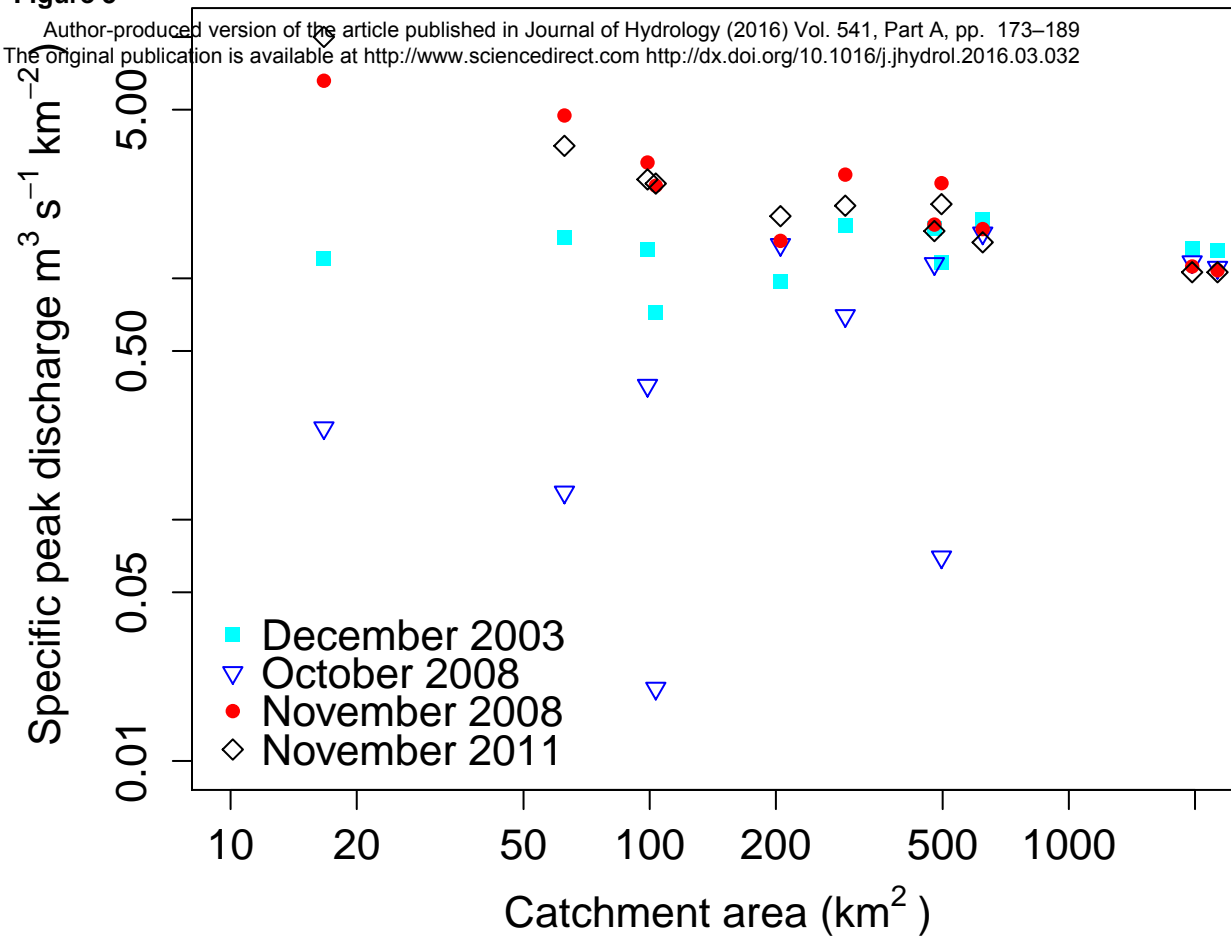


Figure 6

Author-produced version of the article published in Journal of Hydrology (2016) Vol. 541, Part A, pp. 173–189
The original publication is available at <http://www.sciencedirect.com> <http://dx.doi.org/10.1016/j.jhydrol.2016.03.032>

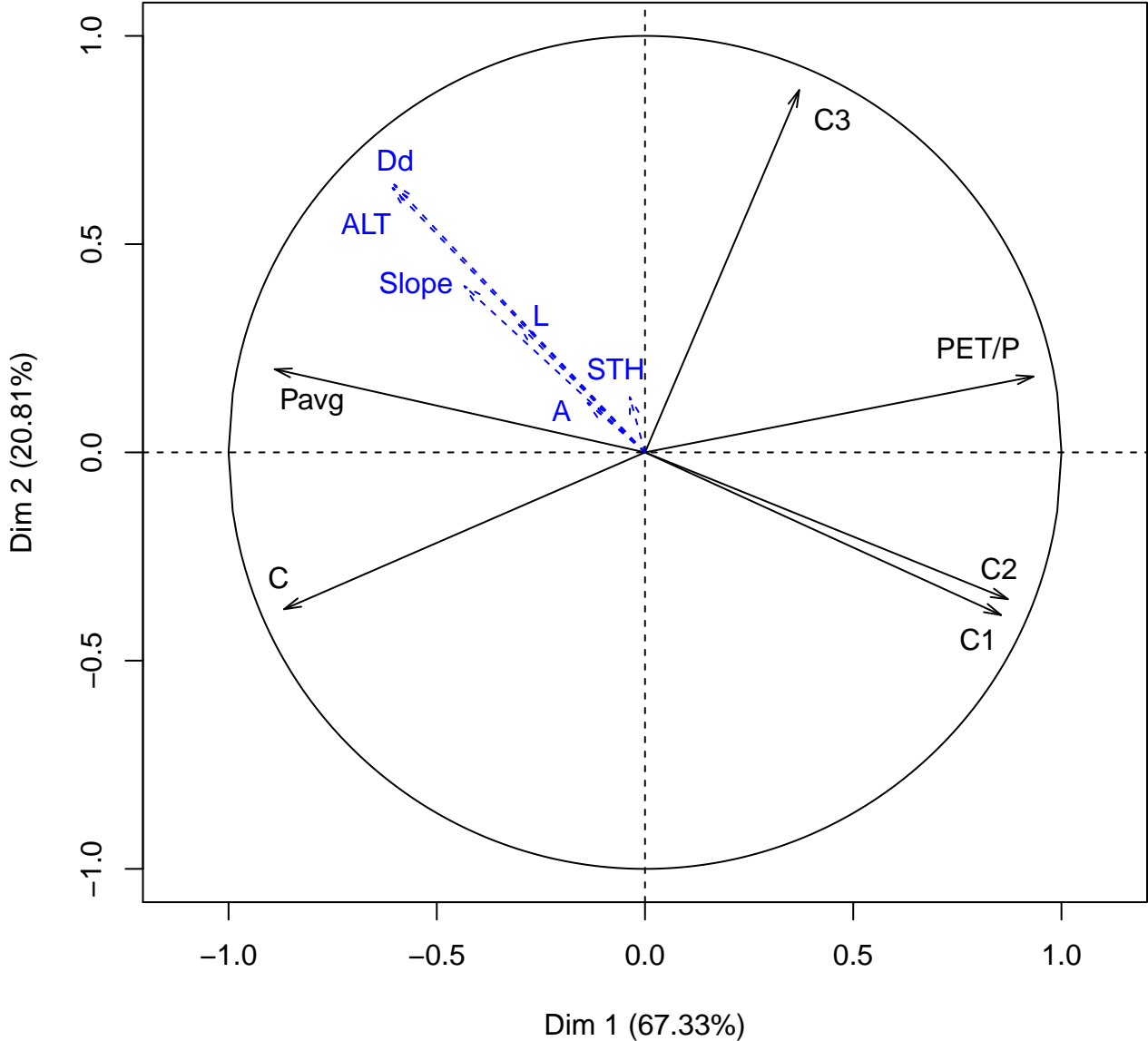
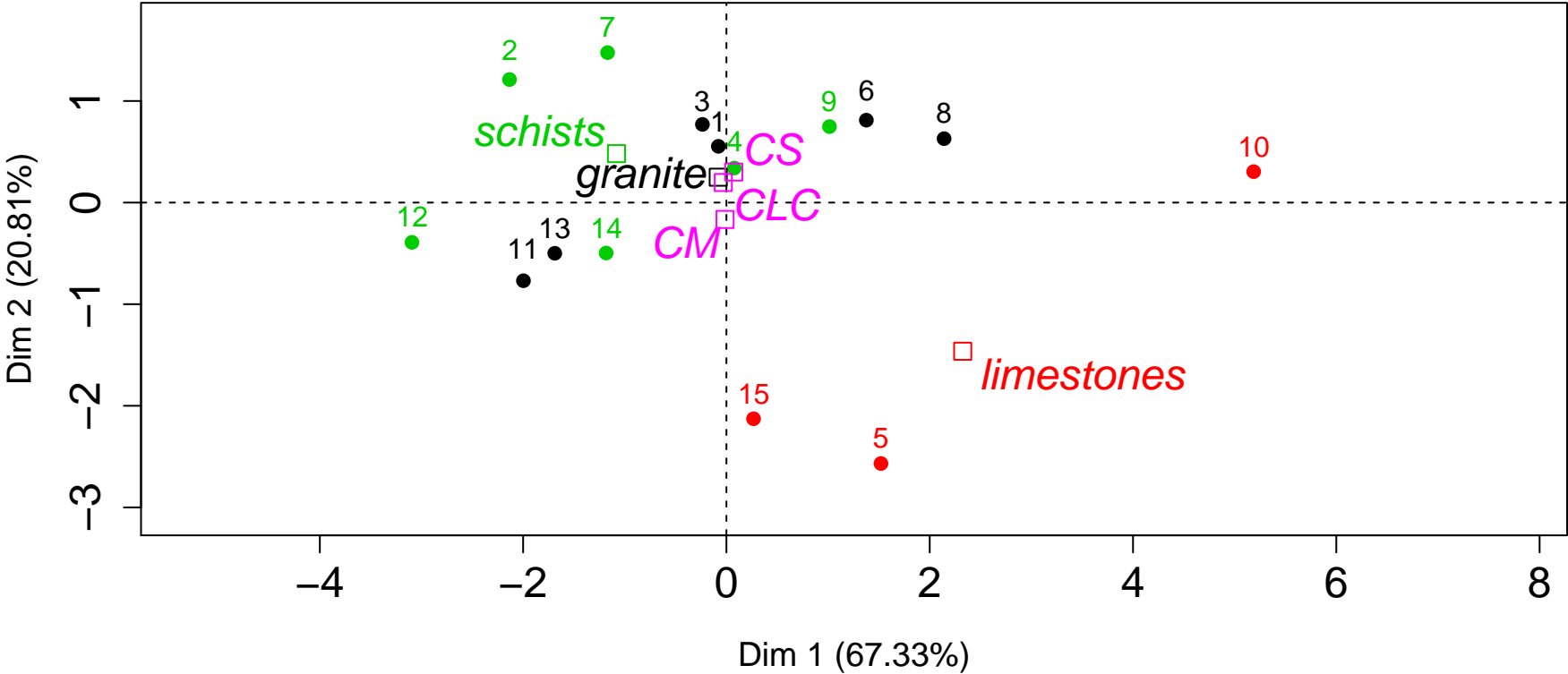
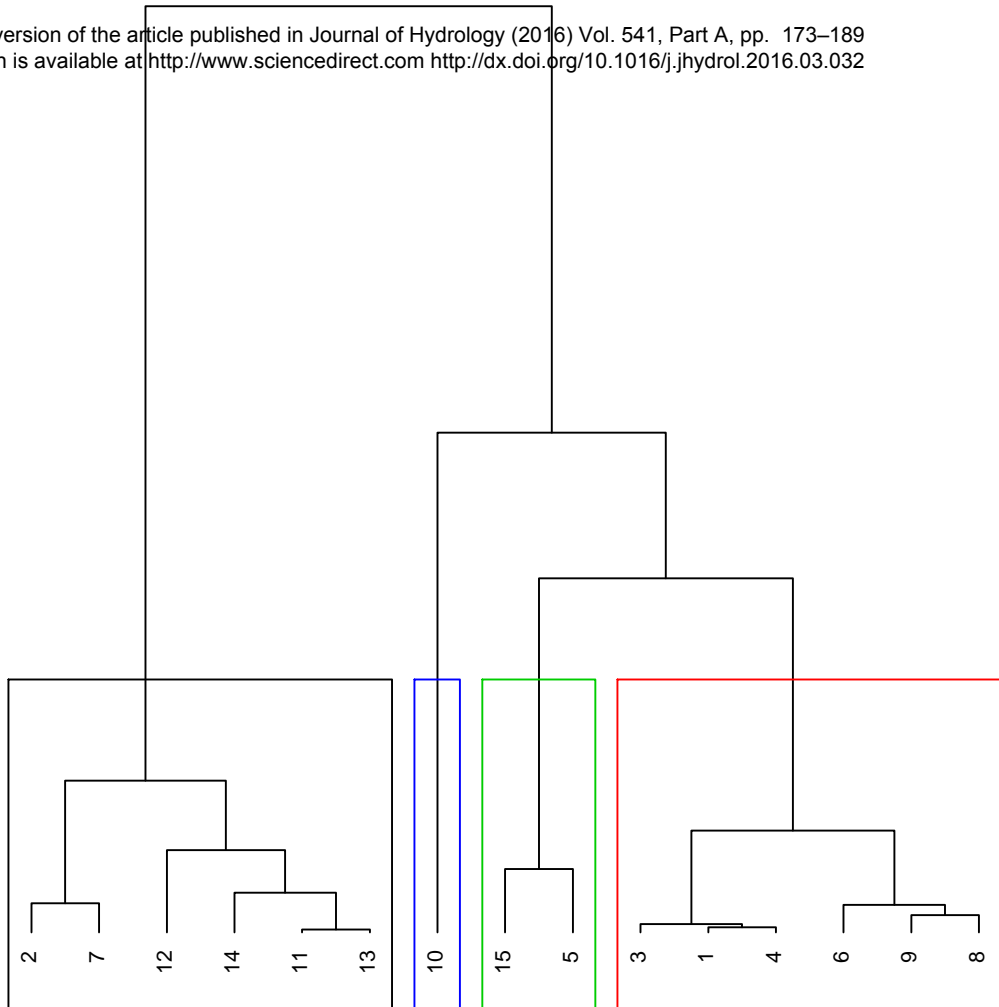


Figure 7

Author-produced version of the article published in Journal of Hydrology (2016) Vol. 541, Part A, pp. 173–189
The original publication is available at <http://www.sciencedirect.com> <http://dx.doi.org/10.1016/j.jhydrol.2016.03.032>



2.0
1.5
1.0
0.5
0.0



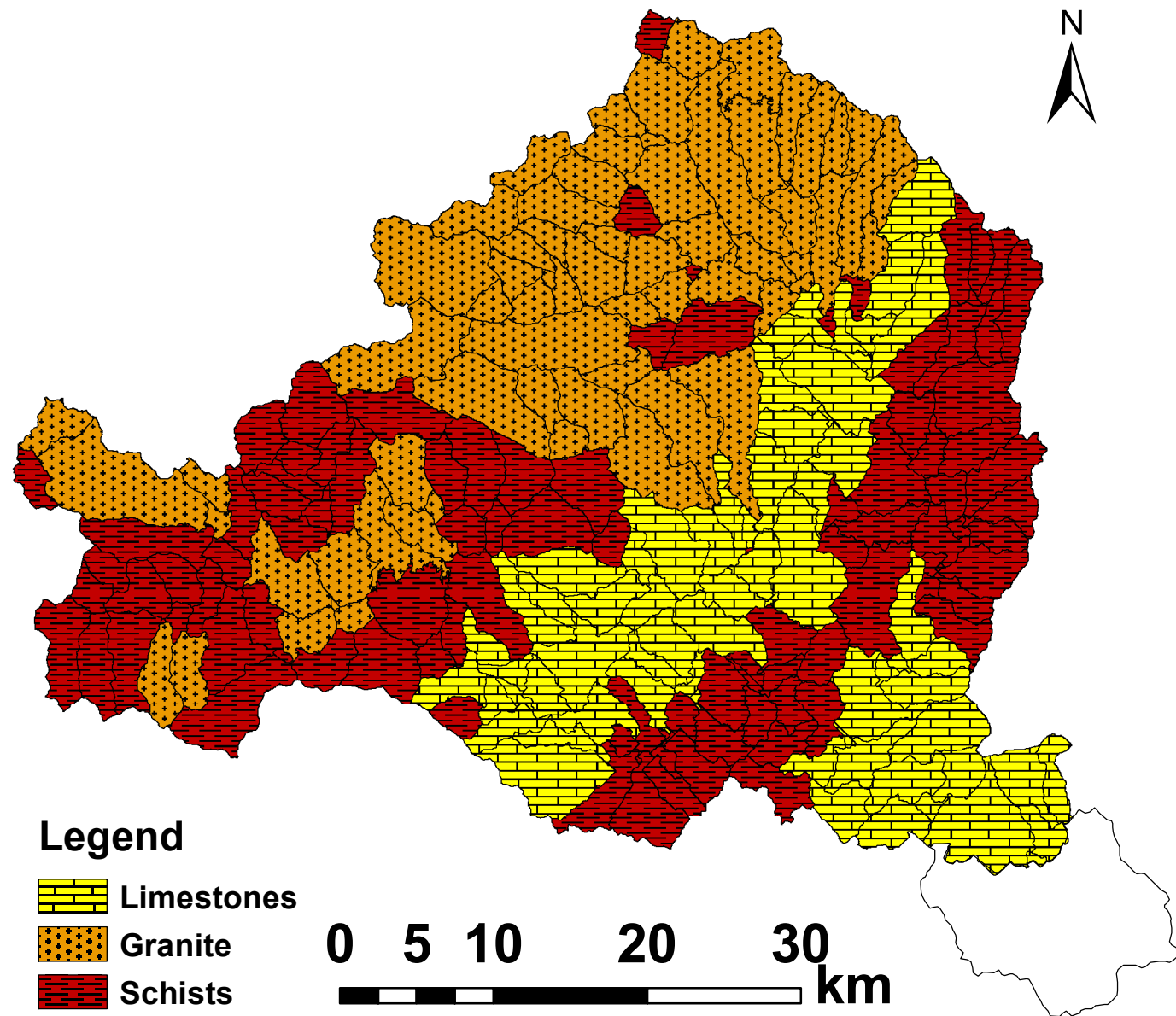


Figure 10

[Click here to download high resolution image](#)

Author-produced version of the article published in Journal of Hydrology (2016) Vol. 541, Part A, pp. 173–189
The original publication is available at <http://www.sciencedirect.com> <http://dx.doi.org/10.1016/j.jhydrol.2016.03.032>

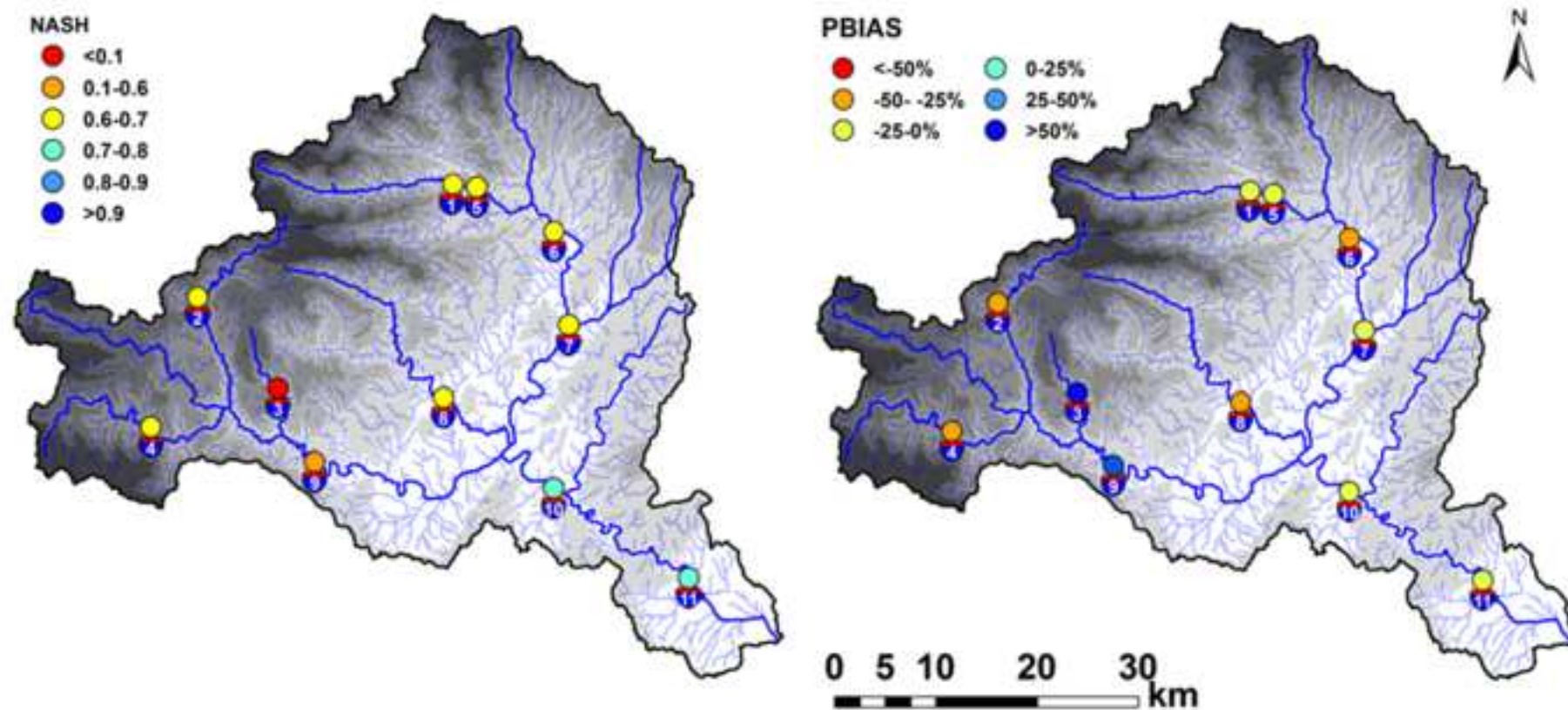


Figure 11

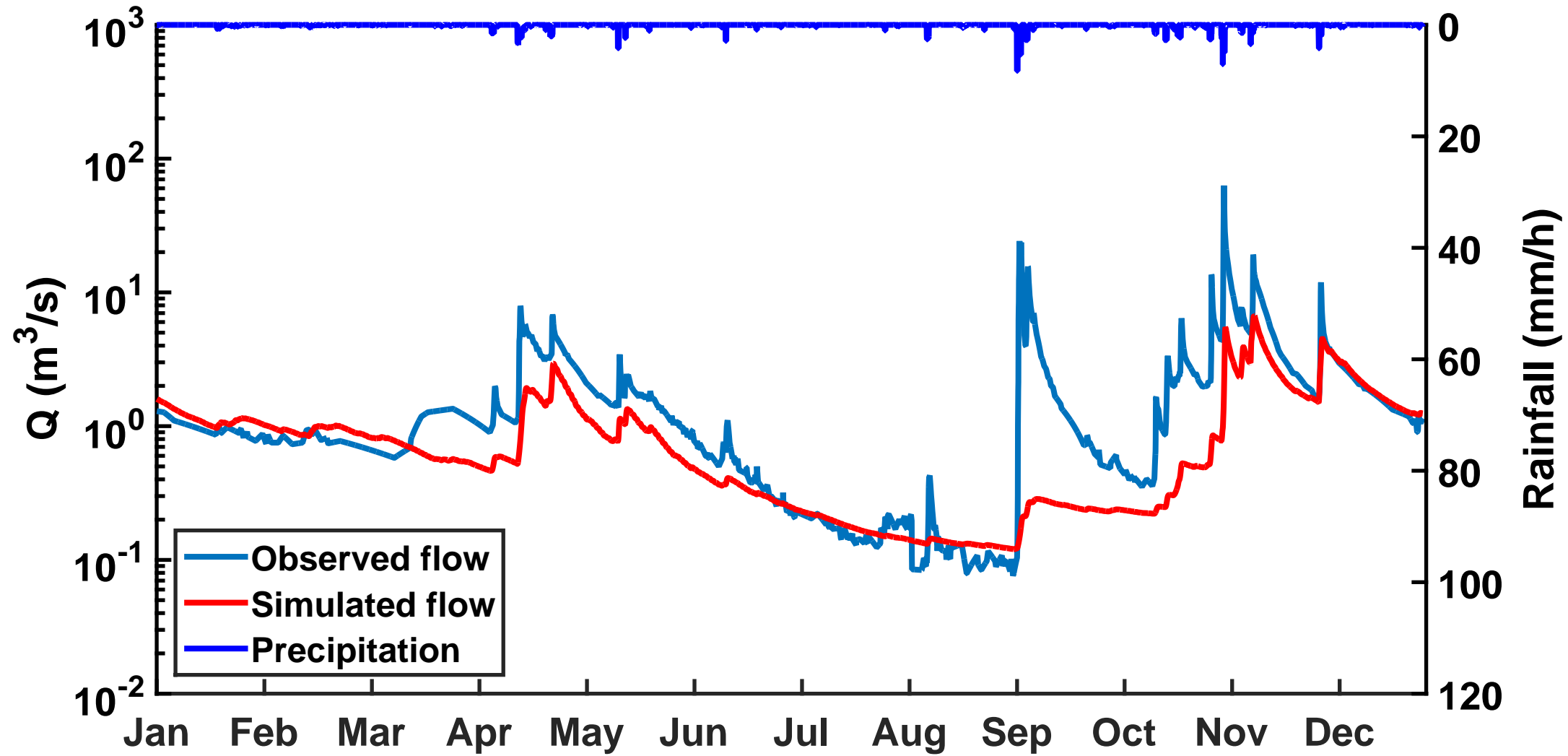
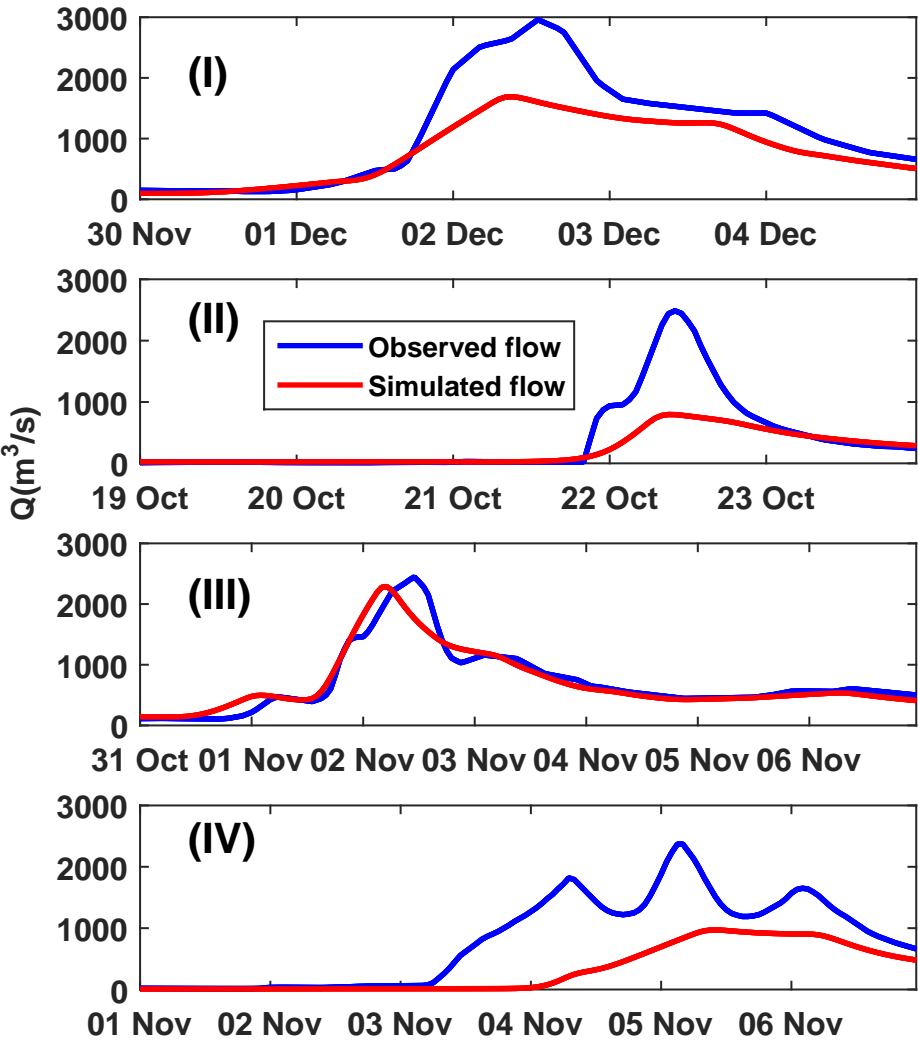


Figure 12



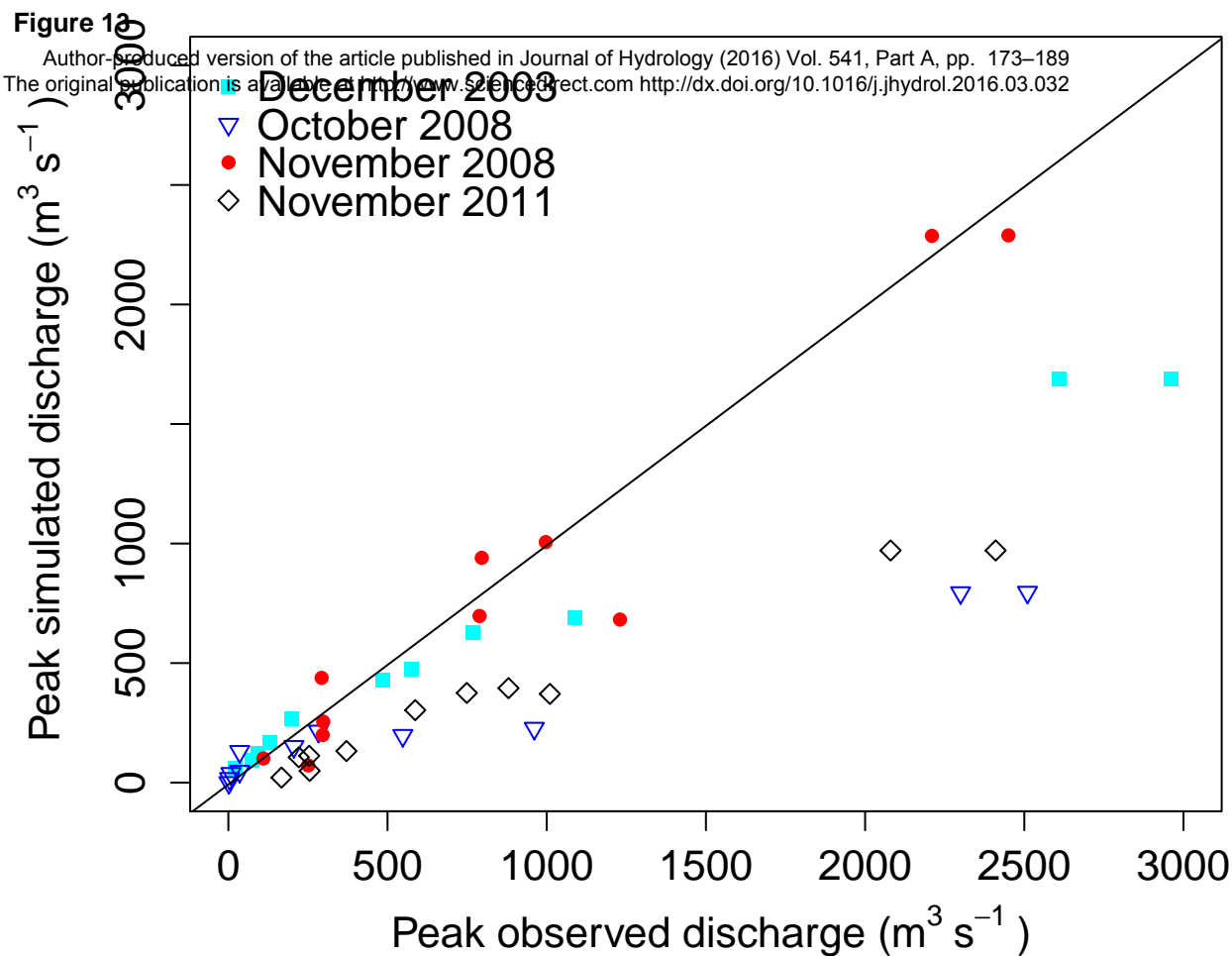


Figure 1. Layout of the SIMPLEFLOOD model applied on each discretized element (in red are new implemented components). Symbols definition is provided in Table 1

Figure 2. Map of the Ardèche catchment with gauging stations and dams position: Source BD TOPO ® IGN database 25 m (in blue: hydrographic network BD CARTHAGE® database)

Figure 3. Geology of the examined area (extracted and processed from geological map of France 1:1 000 000 issued by BRGM (6-th edition, 1996)). The catchments marked in the map are those used for regionalization of model parameters in section 4

Figure 4. Cumulated rainfall averaged over model mesh (a) December 2003 event; b) October 2008; c) November 2008 event and d) November 2011)

Figure 5. Instantaneous specific peak discharge as function of catchment area for the four selected events and selected catchments

Figure 6. Correlation circle of the first two components for our dataset. On the x-axis: dimension 1 / y axis: dimension 2. In black: active variable; in blue: explicative variables

Figure 7. Individual factor map for all catchments (catchments are colored according to different geology and the center of mass of each geology is also drawn on the map)

Figure 8. Hierarchical Clustering Tree of the examined catchments (colors distinguish four clusters)

Figure 9. Geological map of the Ardèche catchment with catchment discretization

Figure 10. Map of the Nash-Sutcliffe efficiencies computed on hourly values and PBIAS for examined stations in the Ardèche catchment for the whole simulation period (2001-2012). For gauges influenced by dams (see Figure 2), comparison is performed using the naturalized discharge.

Figure 11. Comparison of simulated and observed discharge for the Ardèche at Meyras (#1) for year 2005

Figure 12. Comparison of simulated and observed hydrographs at the catchment outlet for selected events (I-December 2003 event; II-October 2008; III- November 2008 event and IV-November 2011)

Figure 13. Comparison of the observed and simulated peak discharge for selected events and examined catchments

